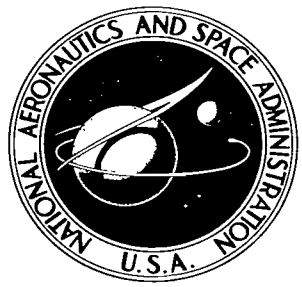

NASA TN D-3781

EFFECTS OF AFT-FUSELAGE-MOUNTED NACELLES ON THE SUBSONIC LONGITUDINAL AERODYNAMIC CHARACTERISTICS OF A TWIN-TURBOJET AIRPLANE

by Lawrence E. Putnam and Charles D. Trescot, Jr.

Langley Research Center
Langley Station, Hampton, Va.

NATIONAL AERONAUTICS AND SPACE ADMINISTRATION • WASHINGTON, D. C. • DECEMBER 1966

NASA TN D-3781

EFFECTS OF AFT-FUSELAGE-MOUNTED NACELLES ON THE SUBSONIC LONGITUDINAL AERODYNAMIC CHARACTERISTICS OF A TWIN-TURBOJET AIRPLANE

By Lawrence E. Putnam and Charles D. Trescot, Jr.

Langley Research Center
Langley Station, Hampton, Va.

NATIONAL AERONAUTICS AND SPACE ADMINISTRATION

For sale by the Clearinghouse for Federal Scientific and Technical Information
Springfield, Virginia 22151 – Price $2.50

EFFECTS OF AFT-FUSELAGE-MOUNTED NACELLES ON THE SUBSONIC LONGITUDINAL AERODYNAMIC CHARACTERISTICS OF A TWIN-TURBOJET AIRPLANE

By Lawrence E. Putnam and Charles D. Trescot, Jr.
Langley Research Center

SUMMARY

An investigation has been made in the Langley 26-inch transonic blowdown tunnel to determine the effects of aft-fuselage-mounted nacelles on the aerodynamic characteristics of a twin-turbojet airplane. The tests were made over a Mach number range from 0.63 to 0.82, at Reynolds numbers (based on wing mean aerodynamic chord) from 2.79×10^6 to 3.94×10^6, and at angles of attack from -2^o to 6^o. The investigation was undertaken primarily to determine the effects of nacelle incidence, nacelle longitudinal location, nacelle cant angle, and modifications to the local area distribution on the lift, drag, and pitching-moment characteristics of the airplane configuration. Some tests were also made in the Langley low-turbulence pressure tunnel at a Mach number of about 0.2 to determine the effects of varying the Reynolds number from 1.36×10^6 to 2.52×10^6 on the high-angle-of-attack (up to 45^o) stability characteristics of the configuration.

Adding nacelles and pylons to the wing-fuselage configuration caused an increase in drag coefficient of approximately 0.0021 at test Mach numbers below 0.76; however, the drag increment decreased with increasing Mach number until the increment was about 0.0007 at a Mach number of 0.82. The nacelles and pylons also caused a reduction in lift coefficient of about 0.09 at a given angle of attack and produced a negative increment in pitching-moment coefficient of approximately 0.04 at a given lift coefficient. Increasing nacelle incidence produced a small decrement in drag coefficient with the maximum decrement occurring for a nacelle incidence of about 2.5^o and also caused small increases in lift and pitching-moment coefficients. The primary effect of moving the nacelles rearward was to increase lift and pitching-moment coefficient so that trim lift coefficient increased 0.07 and 0.13 at Mach numbers of 0.67 and 0.82, respectively. The only significant effect of canting the nacelles 3.5^o (exhaust inward) was a small decrease in drag coefficient at lift coefficients above 0.20. Adding a nacelle fairing to change local area distributions of the basic configuration caused an increase in drag coefficient at Mach numbers below about 0.81; above this Mach number, as a result of favorable interference, there was a small decrease in drag coefficient. Extending the pylons of the modified nacelle configuration caused a reduction in drag coefficient at all test Mach numbers.

INTRODUCTION

At the present time, there is considerable design interest in turbojet airplanes having engines mounted on the rear of the fuselage. The location and alinement of the engine nacelles on the fuselage should have a considerable effect on the drag and performance characteristics of this type of aircraft. Although some theoretical investigations of the effects of aft-mounted nacelles on the aerodynamic characteristics of small turbojet airplanes have been made (for example, refs. 1 and 2), evaluation of nacelle-interference effects can best be determined through experimental studies.

Inasmuch as very few experimental data are generally available, the National Aeronautics and Space Administration has initiated a program to investigate experimentally the effects of aft-fuselage-mounted engine nacelles on the aerodynamic characteristics of a typical twin-turbojet airplane model. The present investigation was undertaken primarily to determine the effects of nacelle incidence, nacelle longitudinal location, and nacelle cant on the lift, drag, and pitching-moment characteristics of the airplane configuration. The effects of horizontal-stabilizer deflection on the aerodynamic characteristics of the airplane have also been investigated. In addition, an investigation has been made to determine the effects on the transonic drag rise of modifying the local area distribution in the region of the nacelles by adding a fairing to the nacelles and by increasing the length of the pylon. The tests were made in the Langley 26-inch transonic blowdown tunnel at Mach numbers from 0.63 to 0.82 and at angles of attack from about -2° to 6°. The Reynolds number (based on wing mean aerodynamic chord) was varied from 2.79×10^6 to 3.94×10^6.

Reference 3 indicates that configurations employing a high-mounted horizontal tail, such as the one on the present configuration, generally have good pitch characteristics at angles of attack prior to wing stall; at angles of attack above stall, however, the effect of the aft-mounted nacelles on the flow over the horizontal tail can have adverse effects on the pitch characteristics of such configurations. Since most of the available data on the problem have been obtained at a relatively low Reynolds number, tests have been made at low subsonic speeds to determine the effects of varying the Reynolds number from 1.36×10^6 to 2.52×10^6 on the aerodynamic characteristics of the present configuration at angles of attack from -4° to 45°. The results of these tests, which were made in the Langley low-turbulence pressure tunnel, are presented in the appendix.

SYMBOLS

The forces and moments are referenced to the stability axes, which have their origin on the fuselage center line and at 20 percent of the mean aerodynamic chord of the wing.

Measurements for this investigation were taken in the U.S. Customary System of Units. Equivalent values are indicated herein parenthetically in the International System (SI). Details concerning the use of SI, together with physical constants and conversion factors, are given in reference 4.

b	wing span
C_D	drag coefficient, $\frac{\text{Drag}}{qS}$
C_L	lift coefficient, $\frac{\text{Lift}}{qS}$
C_m	pitching-moment coefficient, $\frac{\text{Pitching moment}}{qS\bar{c}}$
C_{m_δ}	stabilizer effectiveness parameter obtained over δ_s range from -0.23^o to -1.70^o
C_{L_α}	lift-curve slope per degree
$C_{L,trim}$	trim lift coefficient (that is, lift coefficient at $C_m = 0$)
$\partial C_m / \partial C_L$	longitudinal stability parameter
$\bar{c}$	mean aerodynamic chord
i_n	incidence angle of nacelles, positive when exhaust is downward, degrees
L/D	lift-drag ratio
M_∞	free-stream Mach number
q	dynamic pressure
R	Reynolds number based on $\bar{c}$
S	wing planform area

Δx	longitudinal location of nacelle from basic position, positive rearward
Δx_{cp}	longitudinal location of center of pressure from moment reference center
α	angle of attack, degrees
δ_s	deflection angle of horizontal stabilizer, positive when trailing edge is down, degrees
ϵ	nacelle cant angle, positive when exhaust is inward, degrees

Model-component designations:

B	fuselage
H	horizontal stabilizer
N_1	basic nacelle
N_2	basic nacelle with aft fairing added
P_1	basic pylon
P_2	extended pylon used with N_2
V	vertical tail
W	wing

MODEL

Drawings of the model are shown in figure 1 and photographs of the model are shown as figure 2. The model had a sweptback wing, sweptback horizontal and vertical tails, and aft-fuselage-mounted engine nacelles. Modifications to the rear section of the fuselage were necessary to allow installation of the balance and sting support. A combination aft-fuselage fairing and sting shield was employed to reduce the interference effects. (See bottom photograph in fig. 2.) The gap between the fuselage and the shield was sealed. The wing, which was mounted low on the circular fuselage, had a leading-edge sweep of 33°, an aspect ratio of 5.83, a taper ratio of 0.365, and fences located at 50 percent of the

wing semispan. The all-movable horizontal stabilizer was mounted at about the midpoint of the vertical tail and had provisions for changing the angle of incidence. The pylon-mounted engine nacelles were constructed so as to permit airflow through the circular ducts and were located as shown in figure 1(a). The exit area of the nacelles was 95 percent of the inlet area.

Provisions were made to vary the incidence angle of the nacelles from about 0° to 4° (exhaust downward). The longitudinal location of the nacelles and pylons could also be varied from $\Delta x/\bar{c} = -0.034$ forward of to $\Delta x/\bar{c} = 0.237$ rearward of the nacelle location shown in figure 1(a). Several other modifications were made to the basic nacelle-pylon configuration. One such modification was made by canting the center line of the basic nacelle 3.5° (exhaust inward). (See fig. 1(b).) The basic nacelle was modified by adding a fairing to the aft end of the nacelle (fig. 1(c)). The modified pylon (fig. 1(c)) was obtained by extending the length of the basic pylon.

APPARATUS AND TESTS

The tests were made in the Langley transonic blowdown tunnel which has a slotted octagonal test section measuring 26 inches (66 cm) between flats. The model was mounted on a six-component, internal, strain-gage balance which was sting supported in the tunnel. Model forces and moments were recorded on pen-type strip charts. The base pressure and the pressures necessary to determine Mach number and dynamic pressure were recorded on quick-response flight-type recorders.

All tests of the present investigation were run with fixed transition in order to avoid changes in the aerodynamic forces due to changes in the extent of laminar flow on the model. The 1/16-inch-wide (0.16-cm) transition strips were located on the upper and lower surfaces of the wing, horizontal stabilizer, and nacelle pylons, both sides of the vertical tail, and around the outside and inside of the nacelles. The leading edge of each strip was about 0.2 inch (0.51 cm) behind the leading edge of these model components. The leading edge of the 1/16-inch-wide (0.16-cm) strip on the fuselage was about 0.4 inch (1.02 cm) behind the fuselage nose. All roughness strips were constructed of 0.002-inch-diameter to 0.003-inch-diameter (0.005-cm to 0.008-cm) carborundum grains and a suitable adhesive. The grain size and location of the strips were applied according to the recommendations of reference 5.

The basic configuration ($BWVHN_1P_1$) with $\delta_s = -0.80^{\circ}$, $i_n \approx 0^{\circ}$, $\Delta x/\bar{c} = 0$, and $\epsilon = 0^{\circ}$ was tested at Mach numbers of about 0.63, 0.67, 0.73, 0.77, and 0.82 through an angle-of-attack range of about -2° to 6°. All other configurations were tested only at Mach numbers of about 0.67, 0.73, 0.77, and 0.82 through an angle-of-attack range of about 1° to 5°. Except for the extended-lift-coefficient-range data, the tests were made

primarily at a stagnation pressure of 40 psia (275.8 kN/m^2) with a resulting Reynolds number (based on the wing mean aerodynamic chord) that ranged from 2.79×10^6 to 3.18×10^6. The extended-lift-coefficient-range data for the basic configuration, however, were obtained at a stagnation pressure of 50 psia (344.7 kN/m^2) corresponding to a Reynolds number that ranged from 3.37×10^6 to 3.94×10^6.

The tests of the various configurations were made generally with the horizontal stabilizer deflected -0.80°. However, some tests were made with stabilizer deflection angles of -0.23° and -1.70° in order to determine the effects of stabilizer deflection on the aerodynamic characteristics. Tests were made to evaluate the effects of the nacelle and pylon on the aerodynamic characteristics of the basic configuration (BWVHN$_1$P$_1$). This was accomplished by testing the configuration with nacelles and pylons off (BWVH), with the nacelles and pylons on but the horizontal and vertical tails off (BWN$_1$P$_1$), and with the wing and body only (BW). (Configuration BW was only tested at $M_\infty = 0.72$.)

The basic nacelles and pylons were tested at incidence angles i_n of 0.06°, 0.84°, 1.85°, 2.35°, and 3.81° (exhaust downward), at a nacelle cant angle ϵ of 0°, and at the nacelle-pylon basic longitudinal position $\Delta x/\bar{c}$ of 0. At this longitudinal location, the basic nacelles and pylons were tested with $\epsilon = 3.5°$ (exhaust inward) and $i_n \approx 0°$. The basic nacelles and pylons were also tested at values of $\Delta x/\bar{c}$ of -0.034, 0.072, and 0.237 with $i_n \approx 0°$ and $\epsilon = 0°$. Tests were made on two configurations having modifications to the local area distribution in the region of the nacelles. These modifications to the local area distribution were obtained by modifying the nacelle and the pylon. The modified nacelle was tested with the basic pylon and with the modified pylon.

In order to evaluate the effects of the sting shield (fig. 2), one configuration was tested without the sting shield.

ACCURACY AND CORRECTIONS

Based upon balance accuracy, the estimated maximum values of random errors in the force and moment coefficients, Mach number, and angle of attack are

C_L	±0.003
C_D	±0.0004
C_m	±0.003
M_∞	±0.01
α, deg	±0.1

The angle of attack has been corrected for sting and balance deflection due to aerodynamic loads. The drag data have been adjusted to a condition of free-stream static

pressure at the base of the model sting shield. In addition, the drag coefficient data have been corrected for the calculated internal drag coefficient of the nacelles. The internal skin-friction coefficient of the nacelles was calculated for a ratio of exit area to inlet area of 0.95 by using the following assumptions: (1) The total pressure in the duct was equal to free-stream total pressure, (2) the Mach number at the duct entrance was equal to the free-stream Mach number for duct-exit Mach numbers less than unity, (3) the Mach number at the duct entrance was constant after a duct-exit Mach number of unity was reached, and (4) the duct Mach number was the average of the inlet and exit Mach numbers. From the method of reference 6 and the preceding assumptions, the internal drag coefficient of the nacelles is approximately 0.0010 cos α. No attempt was made to evaluate the pressure components of the internal drag of the nacelles.

For a given Mach number, the drag coefficients obtained at a stagnation pressure of 50 psia (344.7 kN/m^2) would not be comparable to that obtained at a stagnation pressure of 40 psia (275.8 kN/m^2) due to the higher Reynolds number and lower skin-friction coefficients. Therefore, the measured drag coefficients obtained at a stagnation pressure of 50 psia (344.7 kN/m^2) have been increased by an amount equal to the difference in calculated skin-friction drag coefficients between the 40-psia and 50-psia (275.8-kN/m^2 and 344.7-kN/m^2) tests. At both stagnation pressures, the method of reference 6 was employed to calculate the skin-friction coefficients.

Modifications to the rear section of the fuselage were necessary to allow installation of the balance and sting support. As a result of the upsweep of the fuselage in this region, the required balance cavity necessitated a rather large opening that was inclined to the fuselage longitudinal axis. (See fig. 1.) The large variation in pressures across this opening would make any base-pressure corrections to drag coefficient questionable. In order to provide a specified area normal to the model longitudinal axis over which the base-pressures corrections could be more accurately determined, a combination aft-fuselage fairing and sting shield has been employed. (See fig. 2.) It is obvious that this shield may also affect the lift and pitching moment of the model. To obtain an indication of these effects, one configuration was tested with and without the sting shield. The results of these tests indicated that the sting shield has no significant effects on lift coefficient and causes only a small positive increment of approximately 0.005 in pitching-moment coefficient without significantly affecting the longitudinal stability of the configuration.

PRESENTATION OF RESULTS

The basic longitudinal force and moment data at Mach numbers of 0.63 to 0.82 are presented in figures 3 to 18 as shown in the following table:

Figure	Configuration	δ_s, deg	i_n, deg	$\Delta x/\bar{c}$	ϵ, deg
3	BWVH	-0.80			
4	$BWVHN_1P_1$	-.23	0.06	0	0
5 and 6	$BWVHN_1P_1$	-.80	.06	0	0
7	$BWVHN_1P_1$	-1.70	.06	0	0
8	$BWVHN_1P_1$	-.80	.84	0	0
9	$BWVHN_1P_1$	-.80	1.85	0	0
10	$BWVHN_1P_1$	-.80	2.35	0	0
11	$BWVHN_1P_1$	-.80	3.81	0	0
12	$BWVHN_1P_1$	-.80	.04	-0.034	0
13	$BWVHN_1P_1$	-.80	.06	.072	0
14	$BWVHN_1P_1$	-.80	.14	.237	0
15	$BWVHN_1P_1$	-.80	-.04	0	3.5
16	$BWVHN_2P_1$	-.80	-.02	0	0
17	$BWVHN_2P_2$	-.80	-.02	0	0
18	$BWVHN_2P_1$	-.80	1.85	0	0

Various summary plots of the longitudinal aerodynamic characteristics are presented in figures 19 to 27 as shown in the following outline:

DISCUSSION

Effects of Basic Nacelle and Pylon Addition

At Mach numbers between 0.67 and 0.76, adding the basic nacelle-pylon combination (N_1P_1) to the fuselage—wing—vertical-tail—horizontal-tail configuration (BWVH) causes an increase in drag coefficient of approximately 0.0021 at a given lift coefficient in the present test range. (See fig. 19.) Almost all of this drag-coefficient increment is due to the skin-friction drag of the nacelles and pylons. The nacelle and pylon skin-friction drag

coefficient as calculated by the Sommer and Short T' method (ref. 6) is 0.0019. Above a Mach number of 0.76, the increment in drag coefficient due to the nacelles and pylons decreases until, at a Mach number of 0.82 and at $C_L = 0.30$, the drag increment is about 0.0007. This increment is less than the predicted skin-friction drag increment and thus indicates that some favorable interference results from the addition of the nacelles at the higher Mach numbers of the present investigation.

Adding the nacelles and pylons to configuration BWVH results in a loss in lift coefficient of about 0.09 throughout the angle-of-attack and Mach number ranges of the present tests. (Compare figs. 3 and 5.) Coupled with this loss in lift coefficient is a reduction in pitching-moment coefficient of approximately 0.04 throughout the present-test lift range. As a result of these reductions in lift and pitching-moment coefficients, a decrease in trim lift coefficient occurs; with the assumed center of gravity located at 20 percent of the wing mean aerodynamic chord, the trim lift coefficient decreases from 0.29 to 0.14 at a Mach number of 0.67 and from 0.34 to 0.13 at a Mach number of 0.82. (See fig. 19.)

From figure 20, it can be seen that the lift decrement due to nacelle addition is slightly greater for the configuration without the vertical and horizontal tails (BW) than the configuration with the vertical and horizontal tails (BWVH). However, for the tail-off configuration, the pitching-moment-coefficient decrement due to nacelle addition is relatively small. This result indicates that the center of pressure of the lift decrement is slightly ahead of the assumed moment reference center for the tail-off configuration. Reference 2 indicates that an engine nacelle located near a wing behind and above its trailing edge would produce an appreciable reduction in the wing lift. The small positive difference in the increment in lift coefficient due to nacelle addition between the tail-off and tail-on configurations indicates that the nacelles cause a decrease in the downwash on the horizontal tail and thereby produce a small positive increment in lift on the horizontal stabilizer. As a result of the long moment arm of the tail, this positive increment in lift coefficient on the tail produces the large decrement in pitching-moment coefficient resulting from adding the nacelles to configuration BWVH.

Effects of Horizontal-Stabilizer Deflection

Decreasing the horizontal-stabilizer deflection angle from -0.23° to -1.70° causes an increase in pitching-moment coefficient of about 0.065 and a decrease in lift coefficient of about 0.03. (Compare figs. 4, 5, 6, and 7.) The stabilizer effectiveness parameter C_{m_δ} is approximately -0.045 per degree for the basic configuration ($BWVHN_1P_1$). The trim lift coefficient increases from 0.04 to 0.32 at a Mach number of 0.67 and increases from 0.02 to 0.37 at a Mach number of 0.82 as a result of the decrease in stabilizer incidence from -0.23° to -1.70°. (See fig. 21(a).)

Changing the stabilizer incidence angle from -0.23° to -1.70° results in an increase in drag coefficient of approximately 0.0005 throughout the Mach number range of the present investigation. As can be seen in figure 21(b), the drag coefficient varies almost linearly with stabilizer deflection.

Effects of Nacelle Arrangement

Variations in nacelle incidence.- At Mach numbers below approximately 0.75, increasing the nacelle incidence from 0.06° to 3.81° produces a relatively small decrement in drag coefficient (fig. 22); the maximum reduction in C_D, approximately 0.0005, occurs for a nacelle incidence of approximately 2.5°. Above a Mach number of about 0.75, the drag decrement due to nacelle incidence is greater. The maximum decrement in drag coefficient also occurs at a nacelle incidence of approximately 2.5° in this Mach number range. For a nacelle incidence of 2.5°, the drag decrement is about 0.0008 at a Mach number of 0.77 and about 0.0010 at $M = 0.82$ (fig. 22(b)).

Increasing the incidence of the nacelles from 0.06° to 3.81° generally produces positive increments in lift coefficient and pitching-moment coefficient. (Compare figs. 5, 8, 9, 10, and 11.) As a result of these positive increments, trim lift coefficient increases approximately 0.03 at a Mach number of 0.67 and approximately 0.04 at a Mach number of 0.82. (See fig. 22(a).) This increase in trim lift coefficient can have a beneficial effect on the drag of the airplane by reducing the trim drag.

In order to determine whether these effects of nacelle incidence are affected by the shape of the nacelle, the configuration with the modified nacelle $BWVHN_2P_1$ was tested with the nacelles at an incidence angle of approximately 0° and at 1.85°. The effects of nacelle incidence on the aerodynamic characteristics of the basic configuration $BWVHN_1P_1$ (fig. 22) and the modified nacelle configuration (fig. 23) are similar; however, the magnitudes of the effects vary somewhat.

Variation in nacelle longitudinal location.- Moving the nacelles rearward from $\Delta x/\bar{c} = -0.034$ to 0.237 on the basic configuration $BWVHN_1P_1$ generally results in a decrease in drag coefficient at a given lift coefficient for all test Mach numbers. (See fig. 24.) Moving the nacelles rearward also causes a small increase in lift coefficient at a given angle of attack and a considerable increase in pitching-moment coefficient at constant C_L. (Compare figs. 5, 12, 13, and 14.) These increases in C_L and C_m result in a substantial improvement in trim lift coefficient (fig. 24(a)) at all test Mach numbers. Moving the nacelles rearward 27.1 percent of the mean aerodynamic chord ($\Delta x/\bar{c}$ from -0.034 to 0.237) results in an increase in trim lift coefficient of 0.07 and 0.13 at Mach numbers of 0.67 and 0.82, respectively. The decrease in trim drag resulting from the favorable increase in trim lift coefficient will augment the decrement in drag coefficient obtained from moving the nacelles rearward.

Variation in nacelle cant angle.- Above a lift coefficient of 0.20, canting the nacelle 3.5° (exhaust inward) produces a small reduction in drag coefficient below a Mach number of approximately 0.75 and above a Mach number of approximately 0.80. (See fig. 25.) At a lift coefficient of 0.25 and at a Mach number of 0.82, the reduction in drag coefficient due to nacelle cant is approximately 0.0010. Between Mach numbers of approximately 0.75 and 0.80, there is essentially no effect of cant on drag coefficient. Canting the nacelle also causes a small increase in trim lift coefficient (fig. 25), which can cause a further reduction in trim drag.

Effects of Area-Distribution Modifications

Reference 7 indicates that local application of area-rule techniques to the nacelle—pylon—aft-fuselage region of the present configuration can reduce the interference drag in this region and thereby reduce the overall configuration drag rise. Improvements in the local area distribution were accomplished by (1) adding a fairing to the rear of nacelle N_1 to form nacelle N_2 which attached to the original pylon P_1 and (2) extending pylon P_1 to form pylon P_2 which was used in conjunction with the nacelle and fairing N_2. (See fig. 1(c) and the local area distributions in fig. 26.) At Mach numbers below about 0.81 (see fig. 27), the addition of the fairing to the basic nacelle configuration causes an increase in drag coefficient for the range of test lift coefficients. This increase in drag coefficient probably results primarily from the increased skin-friction drag resulting from the increased wetted area of the nacelles. However, above a Mach number of 0.81, the improvements in local area distribution cause the configuration with the modified nacelles (configuration $BWVHN_2P_1$) to have a lower drag than the basic configuration $BWVHN_1P_1$. At $M_\infty = 0.82$ and $C_L = 0.25$, this reduction in drag coefficient amounts to about 0.0006. The nacelle fairing has only small effects on the configuration lift and pitching-moment coefficients (compare figs. 5 and 16) and on trim lift coefficient.

The addition of the pylon extension (P_2) to the configuration with the modified nacelle causes a reduction in drag coefficient at all test lift coefficients and Mach numbers (fig. 27). This reduction in drag coefficient probably results from the improvement in the local area distribution and from improvements in the local flow conditions in the nacelle-fuselage channel and over the rear of the fuselage. At lift coefficients of 0.25 and 0.30, the decrement in C_D resulting from the pylon extensions is such that the drag coefficient of configuration $BWVHN_2P_2$ (configuration with extended pylon and modified nacelle) is less than the drag coefficient of the basic configuration $BWVHN_1P_1$. At $M_\infty = 0.82$ and $C_L = 0.25$, the decrement in drag coefficient is approximately 0.0008. At lift coefficients of 0.15 and 0.20, the drag coefficients of configurations $BWVHN_2P_2$ and $BWVHN_1P_1$ are essentially the same. As can be seen in figure 27, extending the pylons had essentially no effect on trim lift coefficient.

Effects of Combining Most Favorable Geometric Parameters

A summary configuration that combined the most favorable nacelle incidence, cant, longitudinal location, and modifications to the local area distributions was not tested because of the unavailability of the model after these parameters were determined. However, the effects of nacelle incidence and cant, nacelle longitudinal location, and the nacelle fairing and pylon extension on the drag coefficient of the configuration should be independent of each other and, in general, decrements in drag coefficient should be additive. At different nacelle longitudinal locations, the most favorable nacelle incidence angle and cant angle may vary owing to changes in the downwash behind the wing. In any case, the combined favorable interference effects on drag coefficient resulting from improvements in nacelle alinement, nacelle longitudinal location, and modifications to the local area distributions should result in a considerable reduction in the transonic drag rise over that obtained for the basic configuration. It appears that the drag coefficient of the basic configuration can be reduced by as much as 0.0020 to 0.0030 at a Mach number of 0.82 by combining the aforementioned modifications.

As mentioned previously, the addition of the nacelles to the configuration causes a large reduction in trim lift coefficient and associated increase in trim drag. Increasing the nacelle incidence, canting the nacelle, and moving the nacelle rearward all cause an increase in trim lift coefficient; whereas, the modifications to the local area distribution cause small reductions in trim lift coefficient. Combining the effects on $C_{L,trim}$ of these geometric modifications should result in an increase in $C_{L,trim}$ and a corresponding decrease in trim drag over the values obtained for the basic configuration.

Stability and Lift-Curve Slope

For the present investigation, there was essentially no effect of nacelle addition, nacelle incidence and cant, nacelle longitudinal location, and modifications to the local area distribution near the nacelle on the stability and lift-curve slope of the configuration. (See figs. 19, 22 to 25, and 27.) Variations in horizontal-stabilizer deflection angle also had essentially no effect on the stability or lift-curve slope of the configuration. (See fig. 21(a).)

SUMMARY OF RESULTS

An investigation has been made in the Langley 26-inch transonic blowdown tunnel to determine the effects of aft-fuselage-mounted nacelles on the aerodynamic characteristics of a twin-turbojet airplane. The effects of nacelle incidence, nacelle cant, nacelle longitudinal location, and modifications to the local area distribution near the nacelle on the aerodynamic characteristics of the configuration were also investigated. The tests were

made at Mach numbers from 0.63 to 0.82 for angles of attack that generally varied from about -2° to 6°. The investigation indicated the following results:

1. Adding the nacelles and pylons to the configuration caused an increase in drag coefficient of approximately 0.0021 (approximately 8 percent) below a Mach number of 0.76; however, as a result of favorable interference due to nacelle addition, this increment decreased with increasing Mach number until the increment was 0.0007 (approximately 2 percent) at a Mach number of 0.82. The nacelles and pylons also caused a reduction in lift coefficient of about 0.09 at a given angle of attack and a decrease in pitching-moment coefficient of approximately 0.04 at a given lift coefficient.

2. Increasing nacelle incidence produced a small decrement in drag coefficient. The maximum reduction in drag coefficient, 0.0005 at Mach numbers below 0.75 and 0.0010 at a Mach number of 0.82, occurred for a nacelle incidence of approximately 2.5°. Increasing nacelle incidence from 0.06° to 3.81° caused small increases in lift and pitching-moment coefficients with a resulting increase in trim lift coefficient of about 0.03 and 0.04 at Mach numbers of 0.67 and 0.82, respectively.

3. Moving the nacelles rearward 27.1 percent of the wing mean aerodynamic chord caused a small decrease in drag coefficient, a small increase in lift coefficient, and a large increase in pitching-moment coefficient so that the trim lift coefficient increased approximately 0.07 and 0.13 at Mach numbers of 0.67 and 0.82, respectively.

4. Canting the nacelles 3.5° (exhaust inward) on the basic configuration produced a small reduction in drag coefficient at lift coefficients above 0.20 without significantly affecting the other aerodynamic characteristics of the configuration.

5. The only significant effect of adding the nacelle fairing to the basic configuration was an increase in drag coefficient at all test lift coefficients and Mach numbers below about 0.81; above this Mach number there was a slight decrease in drag coefficient (approximately 0.0006 at a Mach number of 0.82 and a lift coefficient of 0.25). Extending the pylons on the modified-nacelle configuration reduced the drag coefficient so that it was essentially the same as the drag coefficient of the basic configuration at lift coefficients below 0.20 and was less than the drag coefficient of the basic configuration at lift coefficients of 0.25 and above.

6. Adding the nacelles and pylons, increasing the nacelle incidence, moving the nacelles rearward, canting the nacelles 3.5°, and modifying the local area distributions near the nacelles all had a favorable effect on the transonic drag rise of the configuration. Combining the effects of these geometric variables on drag coefficient indicates that the drag coefficient of the basic configuration with nacelles may be reduced by as much as

0.0020 to 0.0030 by proper selection of nacelle incidence, cant, and longitudinal location and by modifying the local area distributions in the nacelle region.

Langley Research Center,
National Aeronautics and Space Administration,
Langley Station, Hampton, Va., August 24, 1966,
126-13-01-38-23.

APPENDIX

EFFECTS OF REYNOLDS NUMBER ON THE LOW SUBSONIC AERODYNAMIC CHARACTERISTICS OF CONFIGURATIONS BWVH AND $BWVHN_1P_1$ AT ANGLES OF ATTACK FROM -4^o TO 45^o

Introduction

The NASA has undertaken a wind-tunnel research program to investigate the post-stall or high-angle-of-attack behavior of transport airplanes employing aft-fuselage-mounted nacelles and horizontal stabilizers located high on the vertical tail. (See, for example, ref. 3.) The program was undertaken to determine the factors affecting the so-called "deep stall" characteristics of transport airplanes. However, most tests to date have been made at relatively low Reynolds numbers. Therefore, tests have been made at angles of attack from -4^o to 45^o to determine the effects of Reynolds number on the longitudinal aerodynamic characteristics of two of the configurations tested in the main part of this investigation.

Apparatus and Tests

The tests were made in the Langley low-turbulence pressure tunnel in which the test section is 3 by 7.5 feet (0.91 by 2.29 meters). For these tests, forces and moments were measured with an internal six-component strain-gage balance which was sting supported in the tunnel. The tunnel can accommodate tests in air at stagnation pressures from 1 to 10 atmospheres (1 atm = 101.325 kN/m^2) at Mach numbers up to 0.4. The present tests were made at stagnation pressures from about 60 psia (413.7 kN/m^2) to 150 psia (1034.2 kN/m^2) with corresponding Reynolds numbers, based on wing mean aerodynamic chord, that varied from about 1.36×10^6 to 2.52×10^6. Configurations BWVH and $BWVHN_1P_1$ were tested at Mach numbers near 0.2 and at angles of attack from about -4^o to 45^o. The tests were made without fixed transition and without the sting shield used in the high subsonic tests.

Accuracy and Corrections

Estimated accuracy of the coefficients (based on balance accuracy), Mach number, and angle of attack is indicated as follows:

C_L	± 0.01
C_D (at $\alpha = 0^o$)	± 0.003
C_D (at $\alpha = 45^o$)	± 0.009

APPENDIX

C_m . . . . . ±0.01

M_∞ . . . . . ±0.001

α, deg . . . . . ±0.1

The data have not been corrected for the effects of base pressure or for the internal skin-friction drag of the nacelles. Jet-boundary and tunnel-blockage corrections, as determined by methods of references 8 to 10, have been applied to the data. The angle of attack has been corrected for sting and balance deflections due to aerodynamic loads.

Results and Discussion

The effects of Reynolds number on the subsonic aerodynamic characteristics of configuration BWVH ($\delta_S = -0.23^o$) and configuration $BWVHN_1P_1$ ($\delta_S = -0.23^o$, $i_n = 0.06^o$, $\Delta x/\bar{c} = 0$, and $\epsilon = 0^o$) are shown in figures 28 and 29, respectively. The Reynolds number only significantly affects the pitching-moment and drag coefficients of configurations BWVH and $BWVHN_1P_1$ at angles of attack between about 16^o and 22^o. For configuration $BWVHN_1P_1$ appreciable positive increments in pitching-moment coefficient and negative increments in drag coefficient occur in this angle-of-attack region for an increase in Reynolds number from 1.62×10^6 to 2.12×10^6. There is essentially no effect on the pitching-moment and drag coefficients as the Reynolds number is increased further from $R = 2.12 \times 10^6$ to $R = 2.52 \times 10^6$. The large differences in pitching-moment and drag coefficients between $R = 1.62 \times 10^6$ and 2.12×10^6 in this region (i.e., the region where the airplane first stalls) is possibly associated with a leading-edge separation burble on the inboard wing sections. It should be noted that outboard of the wing fences, the wing leading edge is drooped approximately 30^o whereas inboard, the wing leading edge is not drooped. The outboard droop delays wing-tip separation so that the regaining of leading-edge suction in the inboard region with the increase in Reynolds number from 1.62×10^6 to 2.12×10^6 results in the positive increment in pitching-moment coefficient and the negative increment in drag coefficient.

With the present moment-reference-center location (i.e., at 20 percent of the wing mean aerodynamic chord), configuration BWVH ($\delta_S = -0.23^o$, fig. 28) and configuration $BWVHN_1P_1$ ($\delta_S = -0.23^o$, fig. 29) have no trim points in the high angle-of-attack range ($\alpha > 24^o$) at low subsonic Mach numbers. The variation of $\Delta x_{cp}/\bar{c}$ (the center-of-pressure location) with α shown in figure 29 indicates that a rearward center-of-gravity movement of approximately 15 percent mean aerodynamic chord is permissible before the basic configuration $BWVHN_1P_1$ with $\delta_S = -0.23^o$ will have a stable trim point in the high-angle-of-attack region. However, for other values of horizontal-stabilizer angle δ_S, these results will obviously be different.

REFERENCES

1. Moss, G. M.: Some Aerodynamic Aspects of Rear Mounted Engines. J. Roy. Aeron. Soc., vol. 68, no. 648, Dec. 1964, pp. 837-842.

2. Neumark, S.: Lift Due to Interference Between an Aerofoil and an External Non-Lifting Body. Tech. Note No. Aero. 2960, British R.A.E., May 1964.

3. Ray, Edward J.; and Taylor, Robert T.: Effect of Configuration Variables on the Subsonic Longitudinal Stability Characteristics of a High-Tail Transport Configuration. NASA TM X-1165, 1965.

4. Mechtly, E. A.: The International System of Units – Physical Constants and Conversion Factors. NASA SP-7012, 1964.

5. Braslow, Albert L.; and Knox, Eugene C.: Simplified Method for Determination of Critical Height of Distributed Roughness Particles for Boundary-Layer Transition at Mach numbers From 0 to 5. NACA TN 4363, 1958.

6. Sommer, Simon C.; and Short, Barbara J.: Free-Flight Measurements of Turbulent-Boundary-Layer Skin Friction in the Presence of Severe Aerodynamic Heating at Mach Numbers From 2.8 to 7.0. NACA TN 3391, 1955.

7. Kutney, John T.; and Piszkin, Stanley P.: Reduction of Drag Rise of the Convair 990 Airplane. J. Aircraft, vol. 1, no. 1, Jan.-Feb. 1964, pp. 8-12.

8. Katzoff, S.; and Hannah, Margery E.: Calculation of Tunnel-Induced Upwash Velocities for Swept and Yawed Wings. NACA TN 1748, 1948.

9. Swanson, Robert S.; and Toll, Thomas A.: Jet-Boundary Corrections for Reflection-Plane Models in Rectangular Wind Tunnels. NACA Rept. 770, 1943. (Supersedes NACA WR L-458.)

10. Herriot, John G.: Blockage Corrections For Three-Dimensional-Flow Closed-Throat Wind Tunnels, With Consideration of the Effect of Compressibility. NACA Rept. 995, 1950. (Supersedes NACA RM A7B28.)

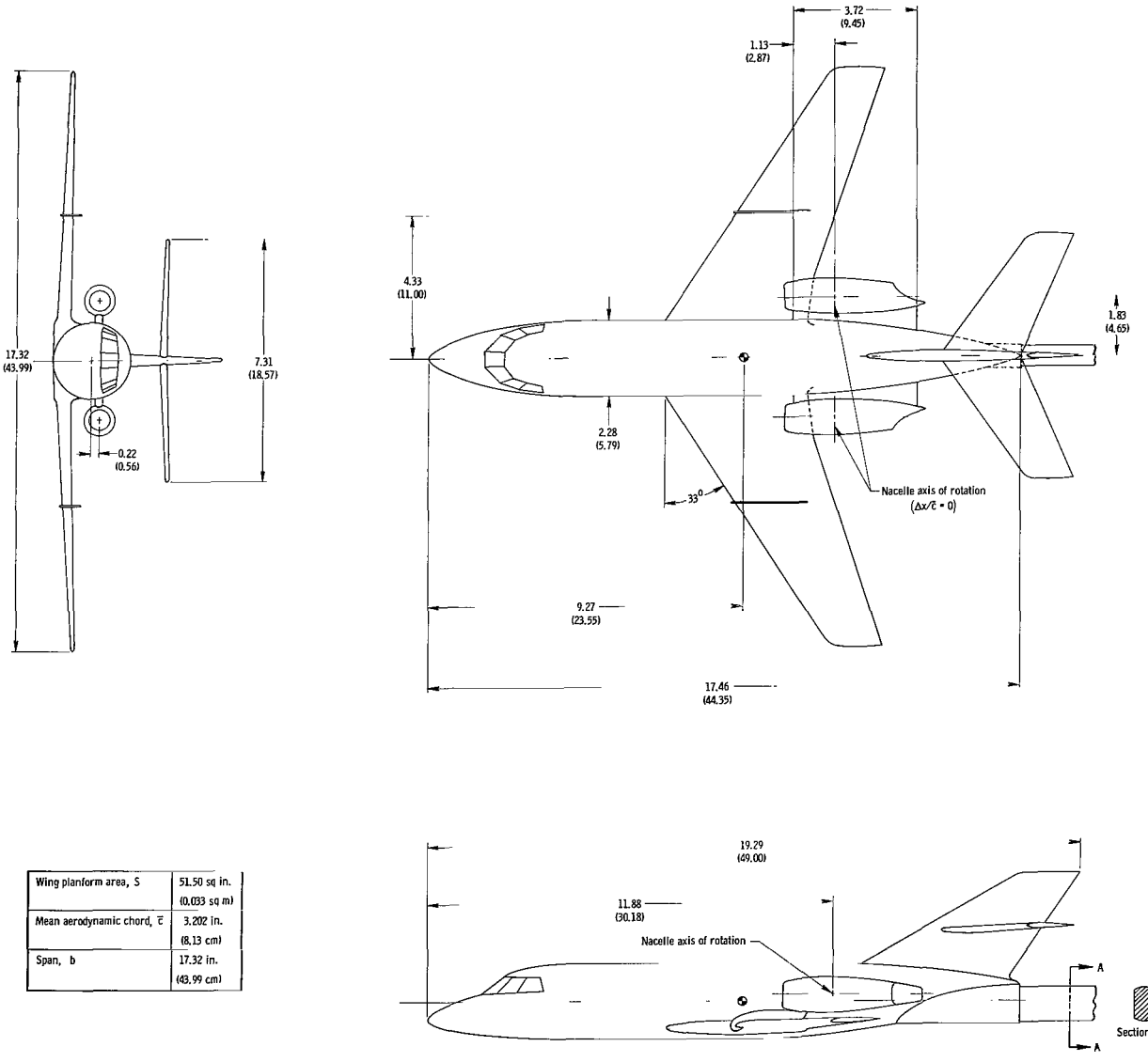

Wing planform area, S	51.50 sq in. (0.033 sq m)
Mean aerodynamic chord, $\bar{c}$	3.202 in. (8.13 cm)
Span, b	17.32 in. (43.99 cm)

(a) Basic configuration $BWVHN_1P_1$.

Figure 1.- Drawings of the model. All linear dimensions are in inches (centimeters).

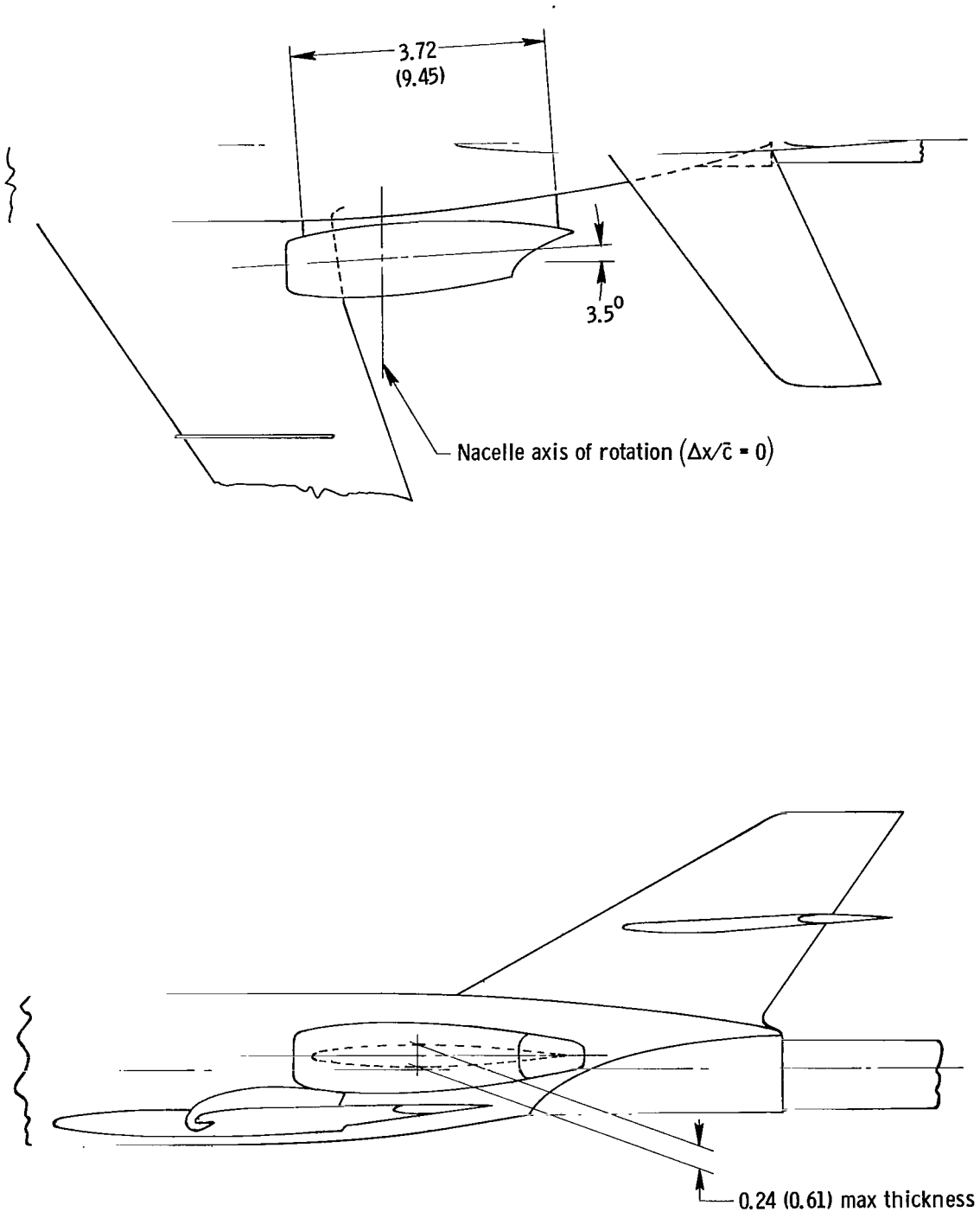

(b) Configuration $BWVHN_1P_1$ with $\varepsilon = 3.5^0$.

Figure 1.- Continued.

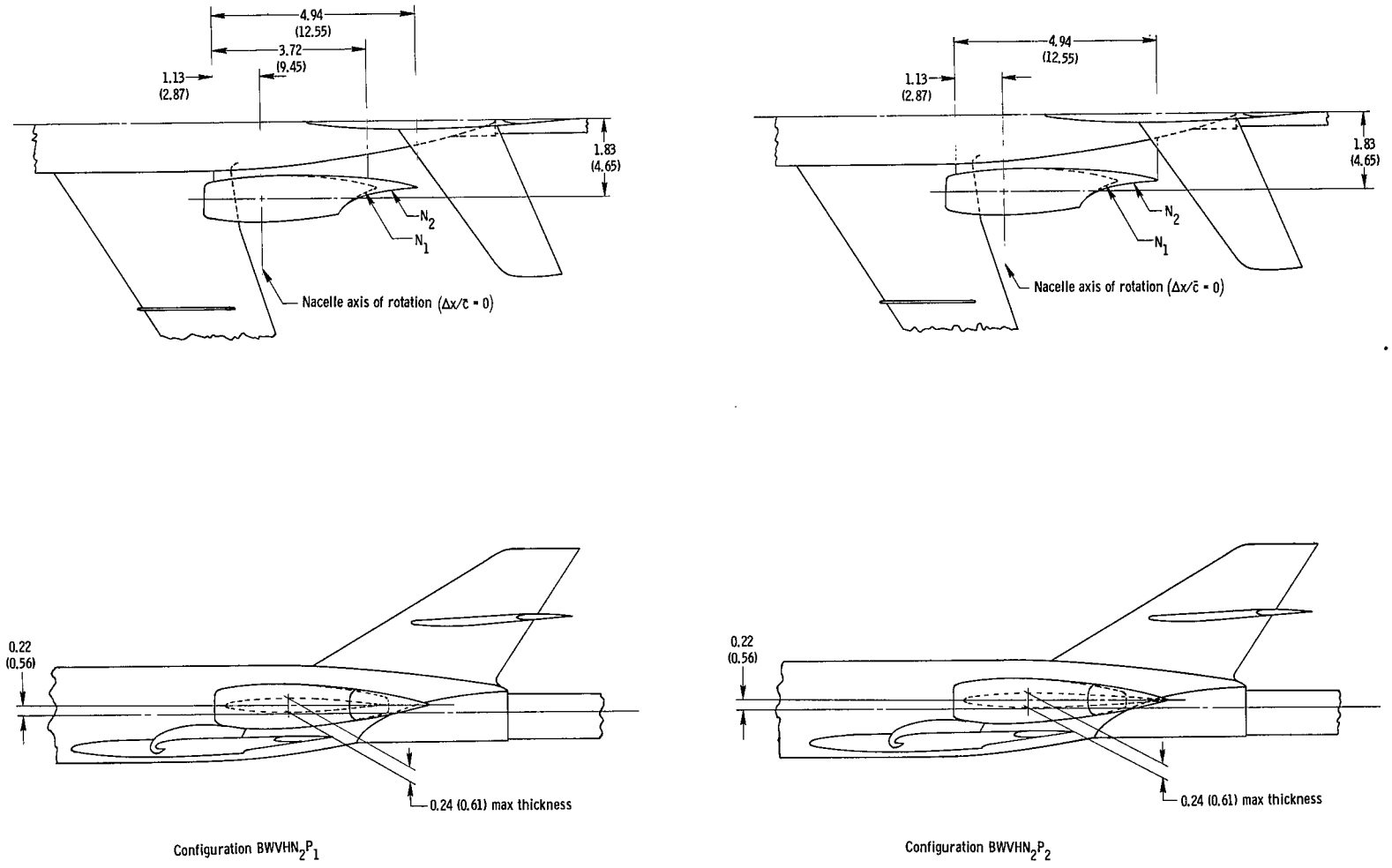

(c) Configurations BWVHN$_2$P$_1$ and BWVHN$_2$P$_2$.

Figure 1.- Concluded.

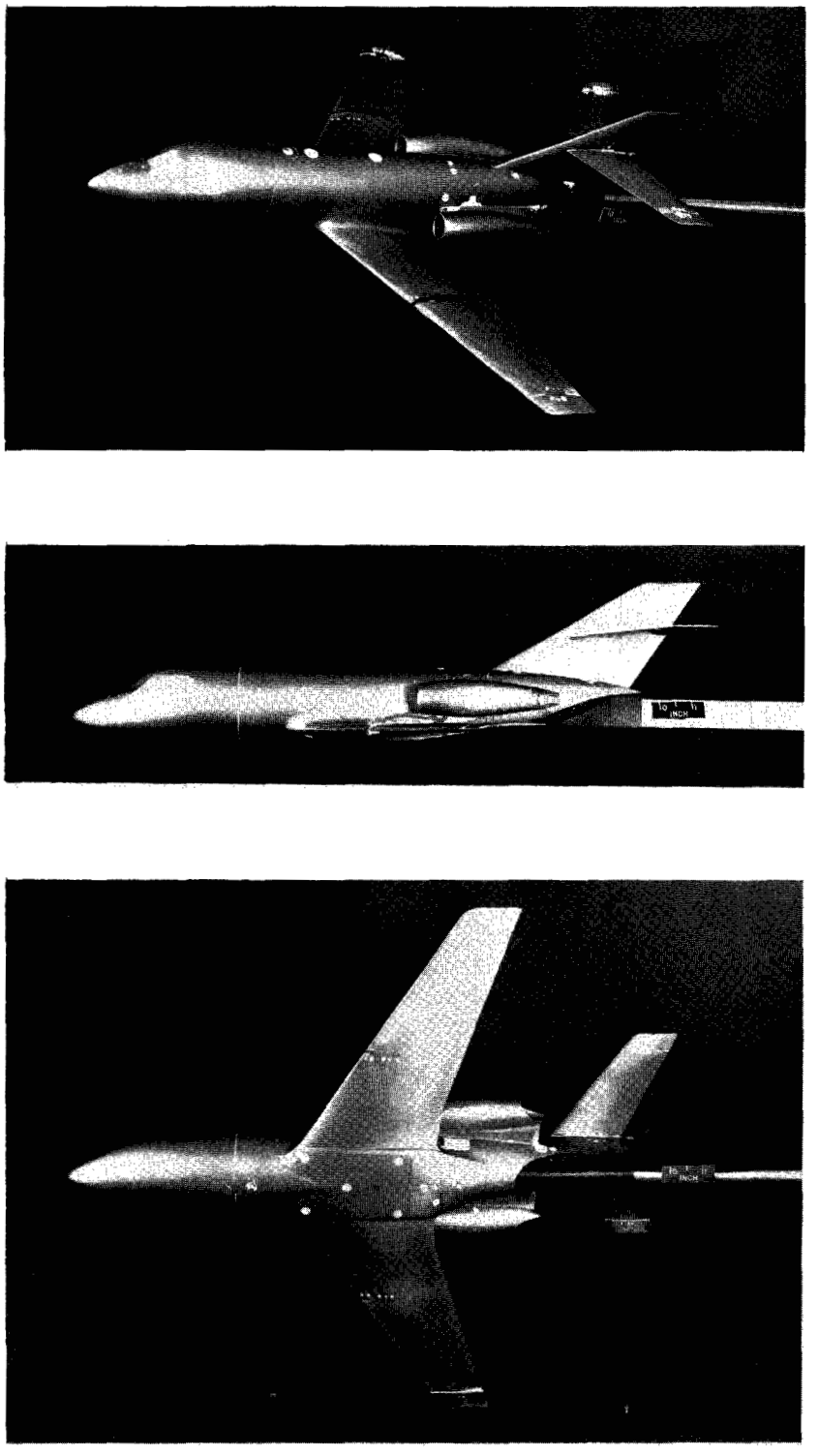

Figure 2.- Photographs of configuration BWVHN$_1$P$_1$ with $\delta_s = -0.80^o$, $i_n = 0.06^o$, $\Delta x/\bar{c} = 0$, and $\varepsilon = 0^o$. L-66-7606

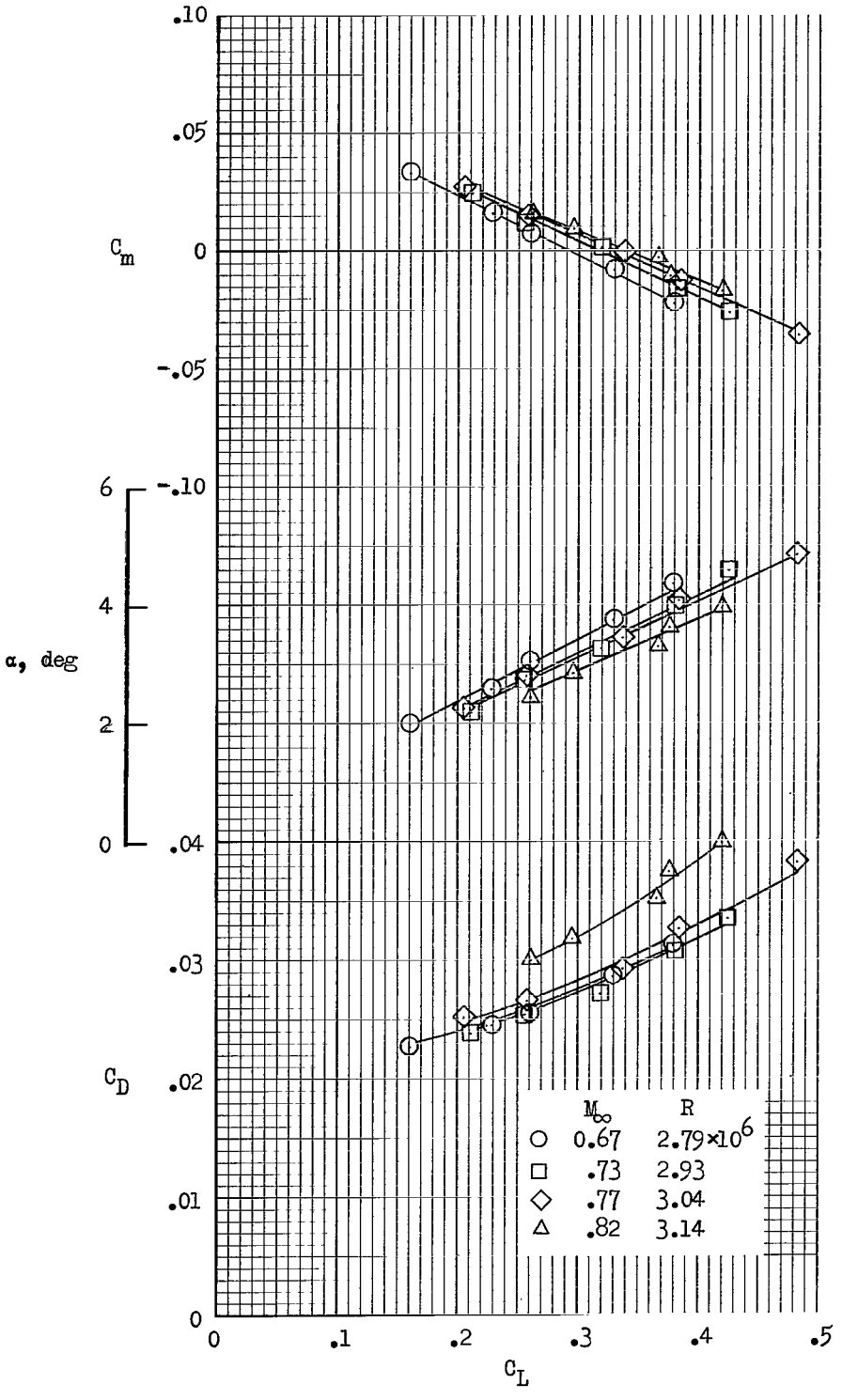

Figure 3.- Longitudinal aerodynamic characteristics of configuration BWVH with $\delta_s = -0.80^o$.

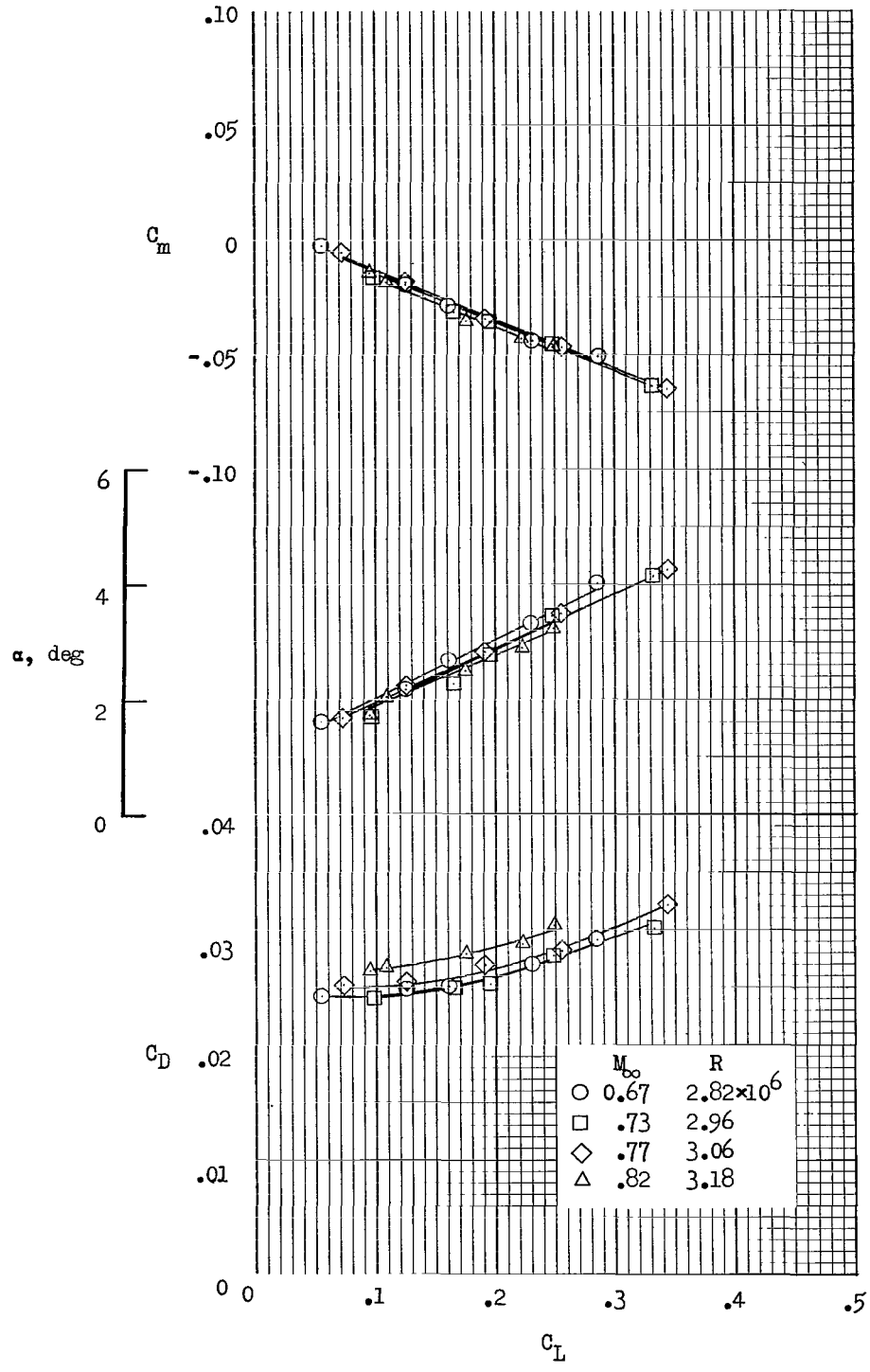

Figure 4.- Longitudinal aerodynamic characteristics of configuration BWVHN$_1$P$_1$ with $\delta_s = -0.23^0$, $i_n = 0.06^0$, $\Delta x/\bar{c} = 0$, and $\varepsilon = 0^0$.

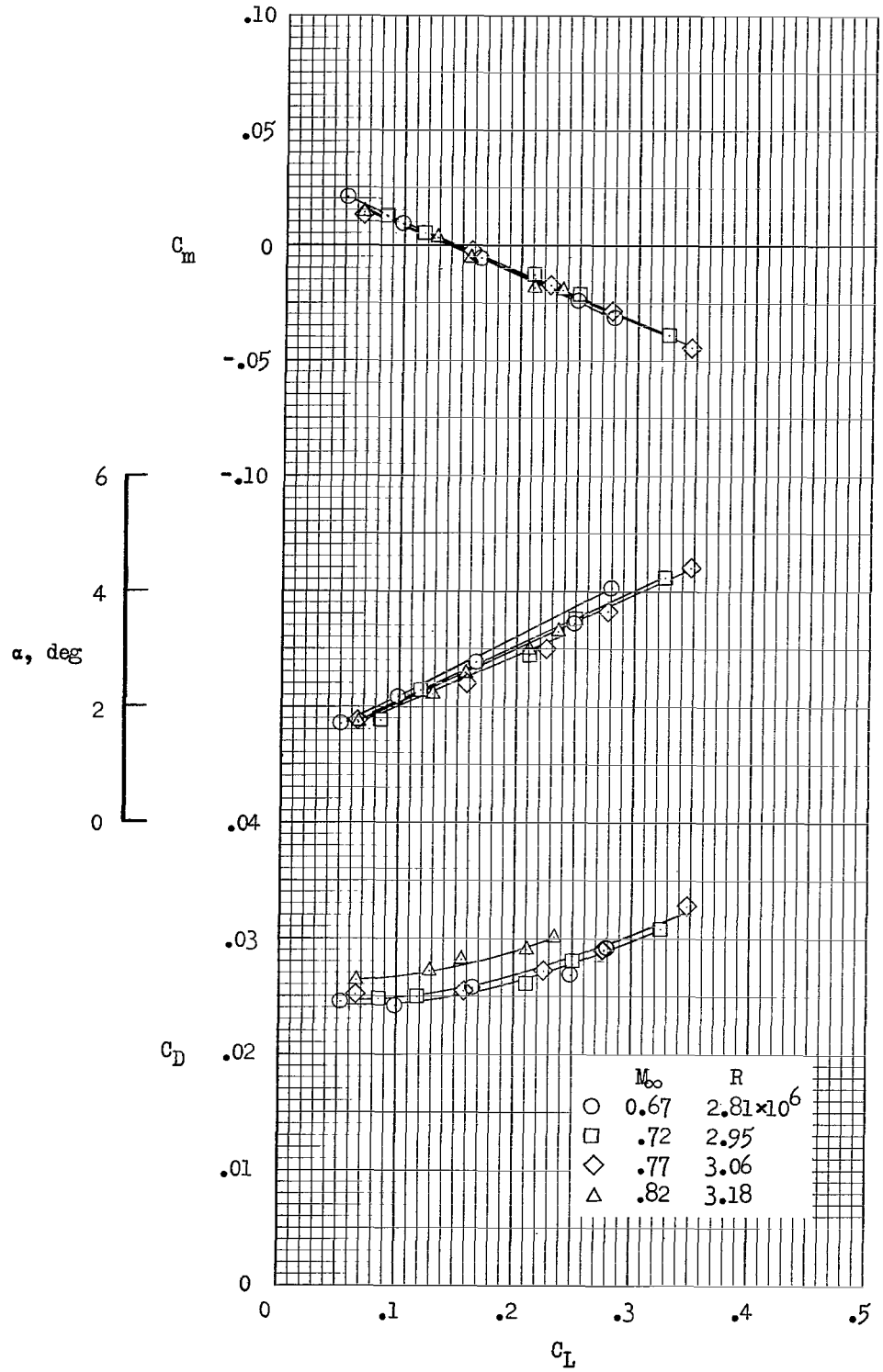

Figure 5.- Longitudinal aerodynamic characteristics of configuration $BWVHN_1P_1$ with $\delta_s = -0.80^0$, $i_n = 0.06^0$, $\Delta x/\bar{c} = 0$, and $\varepsilon = 0^0$.

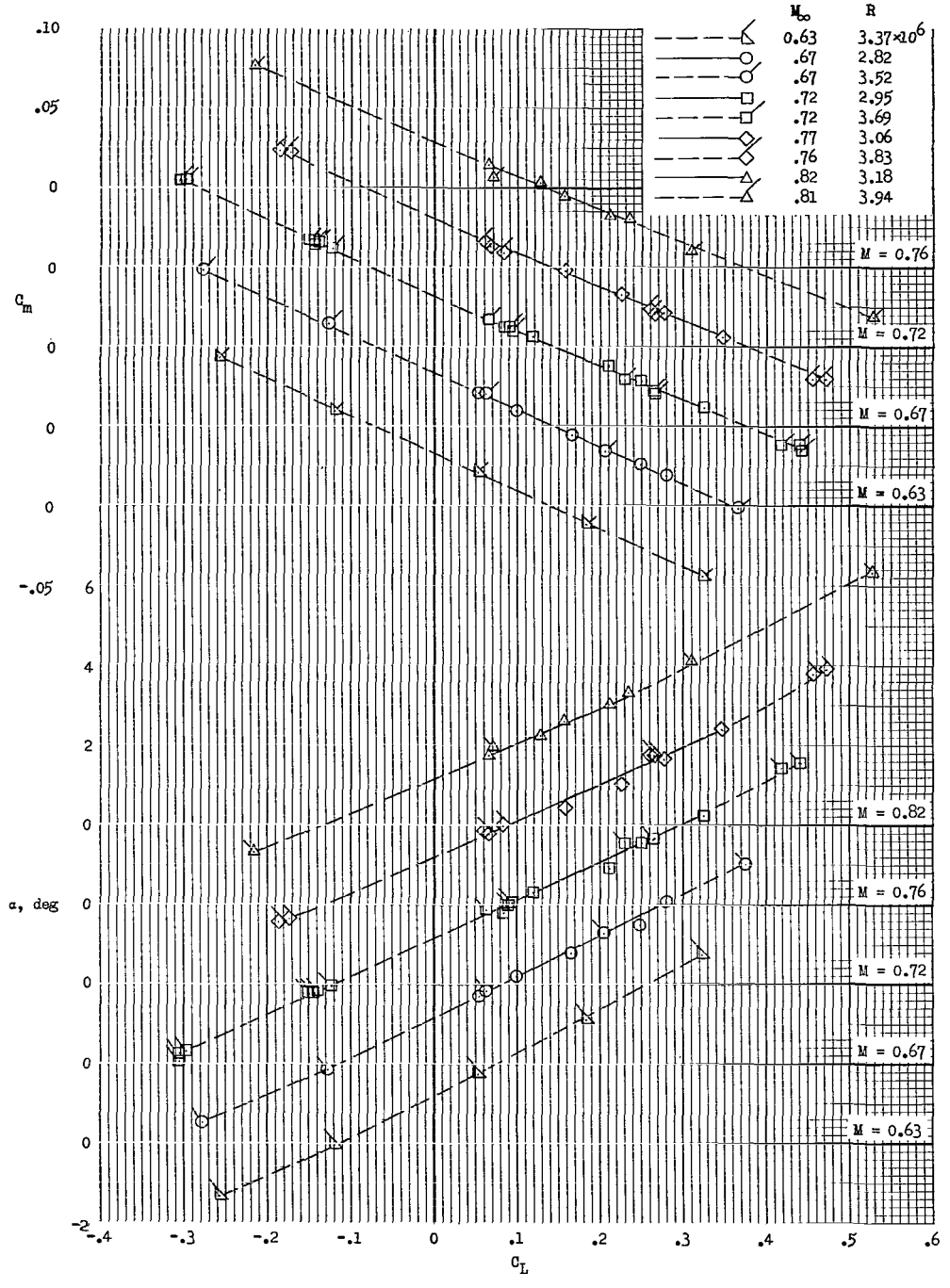

(a) Variation of C_m and α with C_L.

Figure 6.- Longitudinal aerodynamic characteristics of configuration BWVHN$_1$P$_1$ with $\delta_s = -0.80^0$, $i_n \approx 0^0$, $\Delta x/\bar{c} = 0$, and $\varepsilon = 0^0$. Extended lift-coefficient range is $-0.3 \leqq C_L \leqq 0.6$.

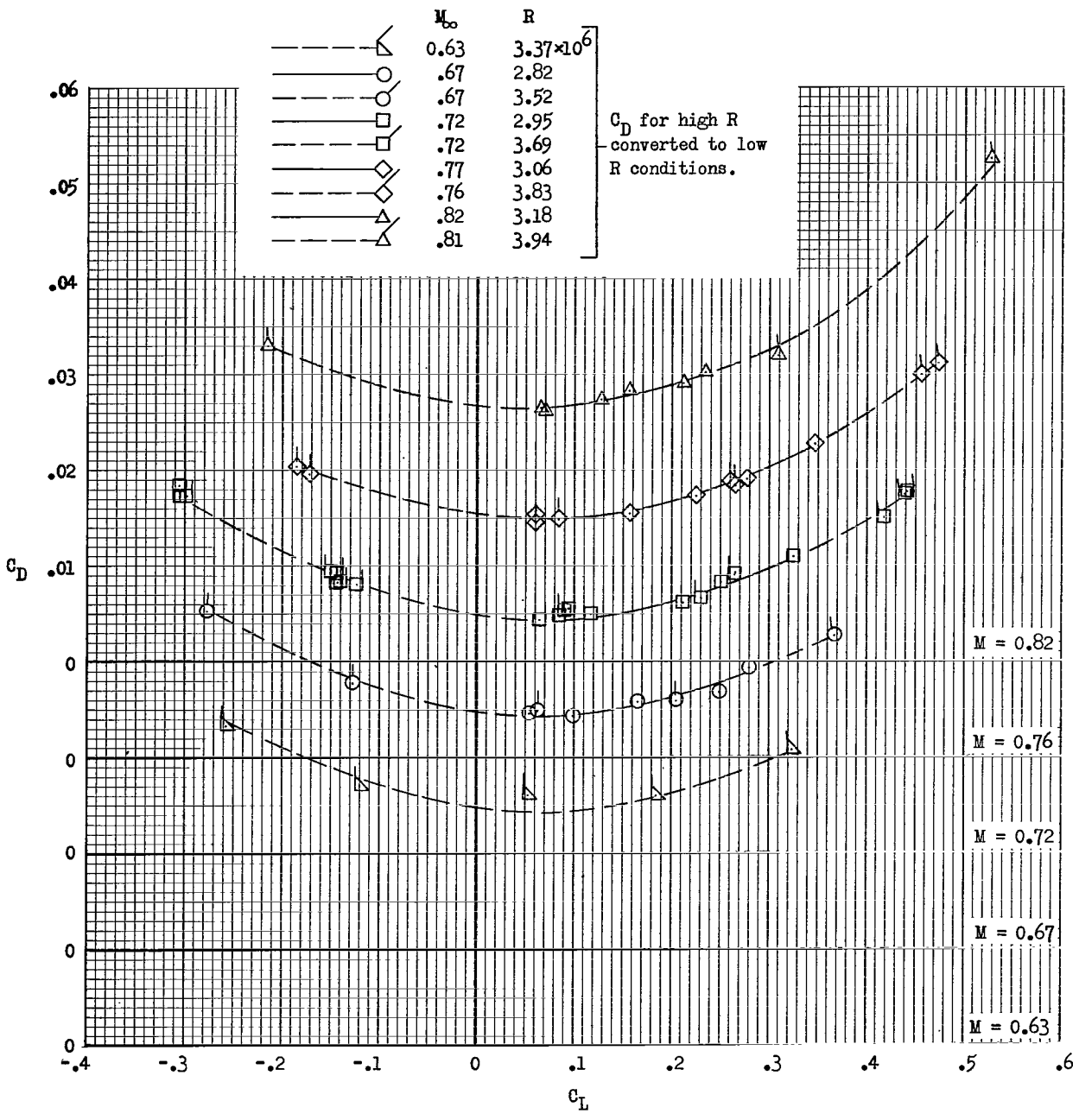

(b) Variation of C_D with C_L.

Figure 6.- Concluded.

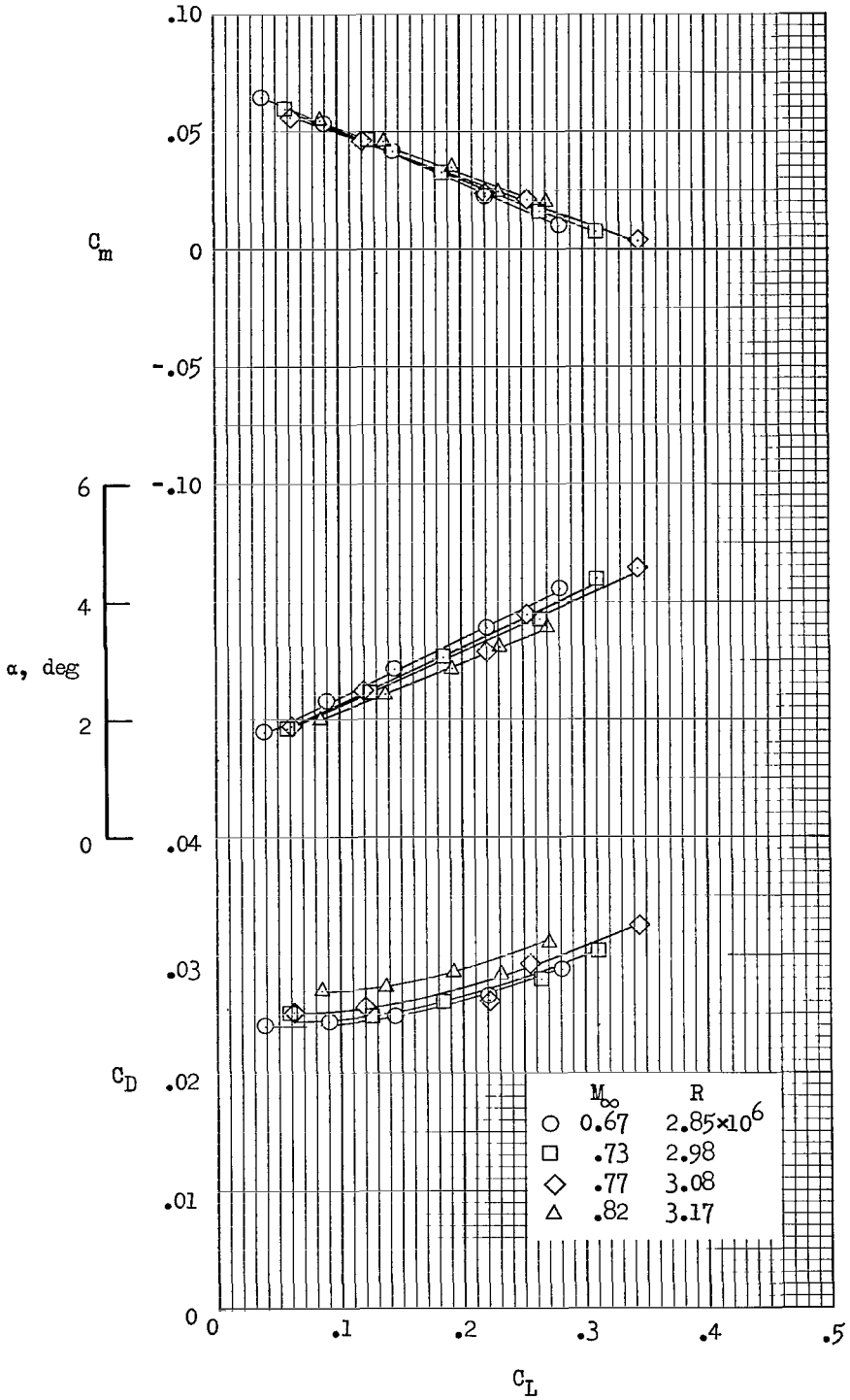

Figure 7.- Longitudinal aerodynamic characteristics of configuration $BWVHN_1P_1$ with $\delta_s = -1.70^0$, $i_n = 0.06^0$, $\Delta x/\bar{c} = 0$, and $\varepsilon = 0^0$.

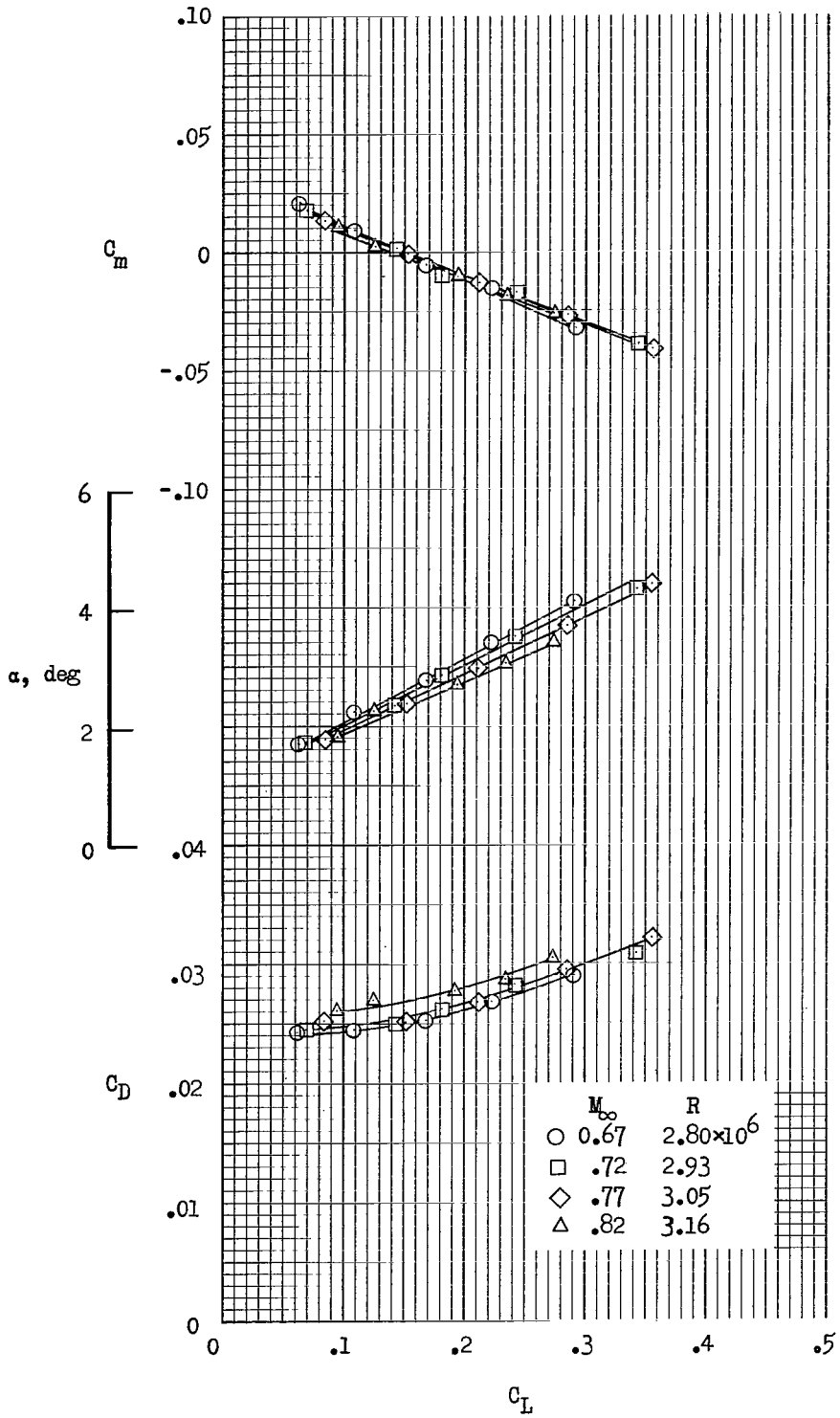

Figure 8.- Longitudinal aerodynamic characteristics of configuration BWVHN$_1$P$_1$ with $\delta_s = -0.80^0$, $i_n = 0.84^0$, $\Delta x/\bar{c} = 0$, and $\varepsilon = 0^0$.

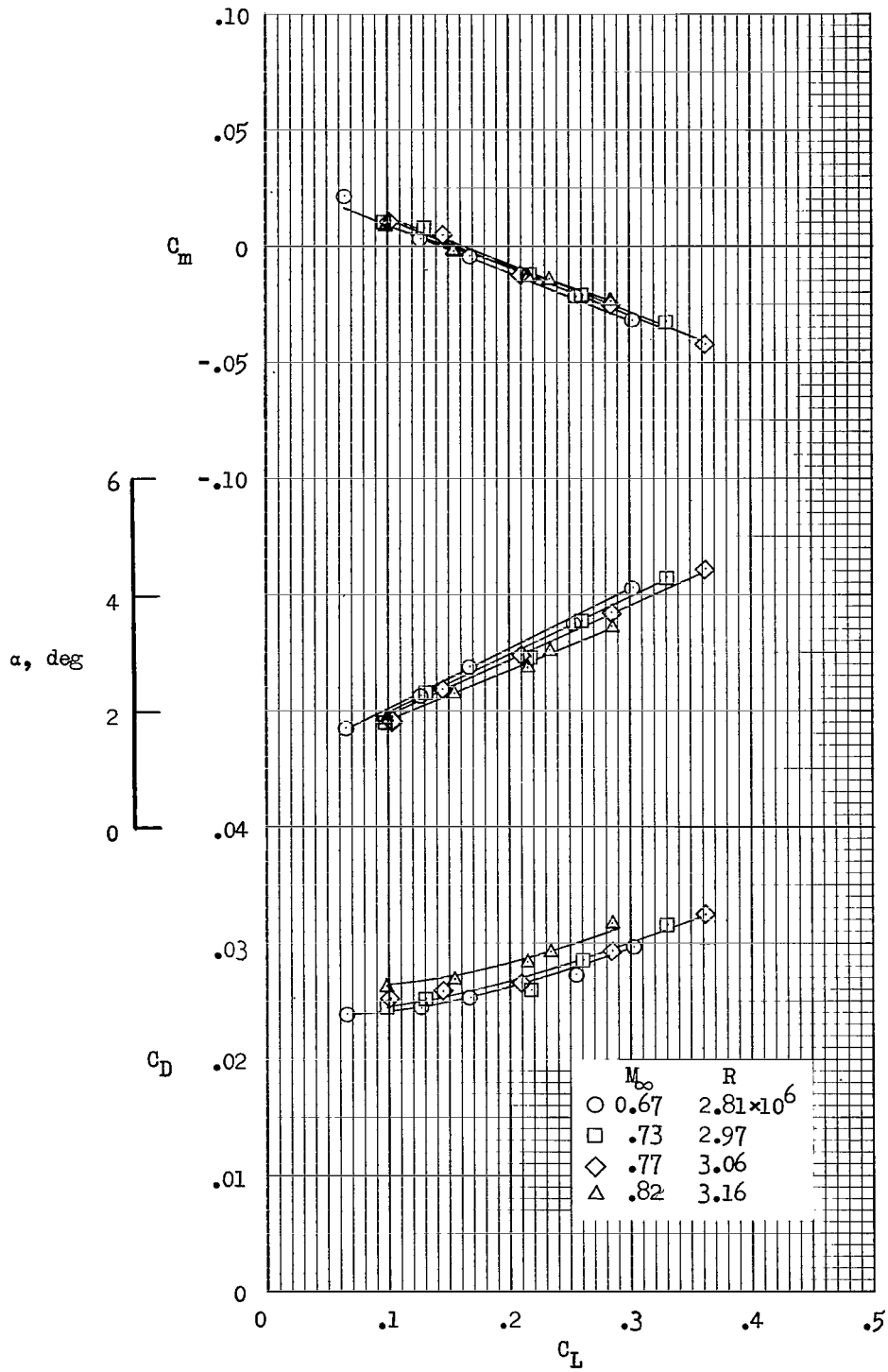

Figure 9.- Longitudinal aerodynamic characteristics of configuration BWVHN1P1 with $\delta_s = -0.80^o$, $i_n = 1.85^o$, $\Delta x/\bar{c} = 0$, and $\varepsilon = 0^o$.

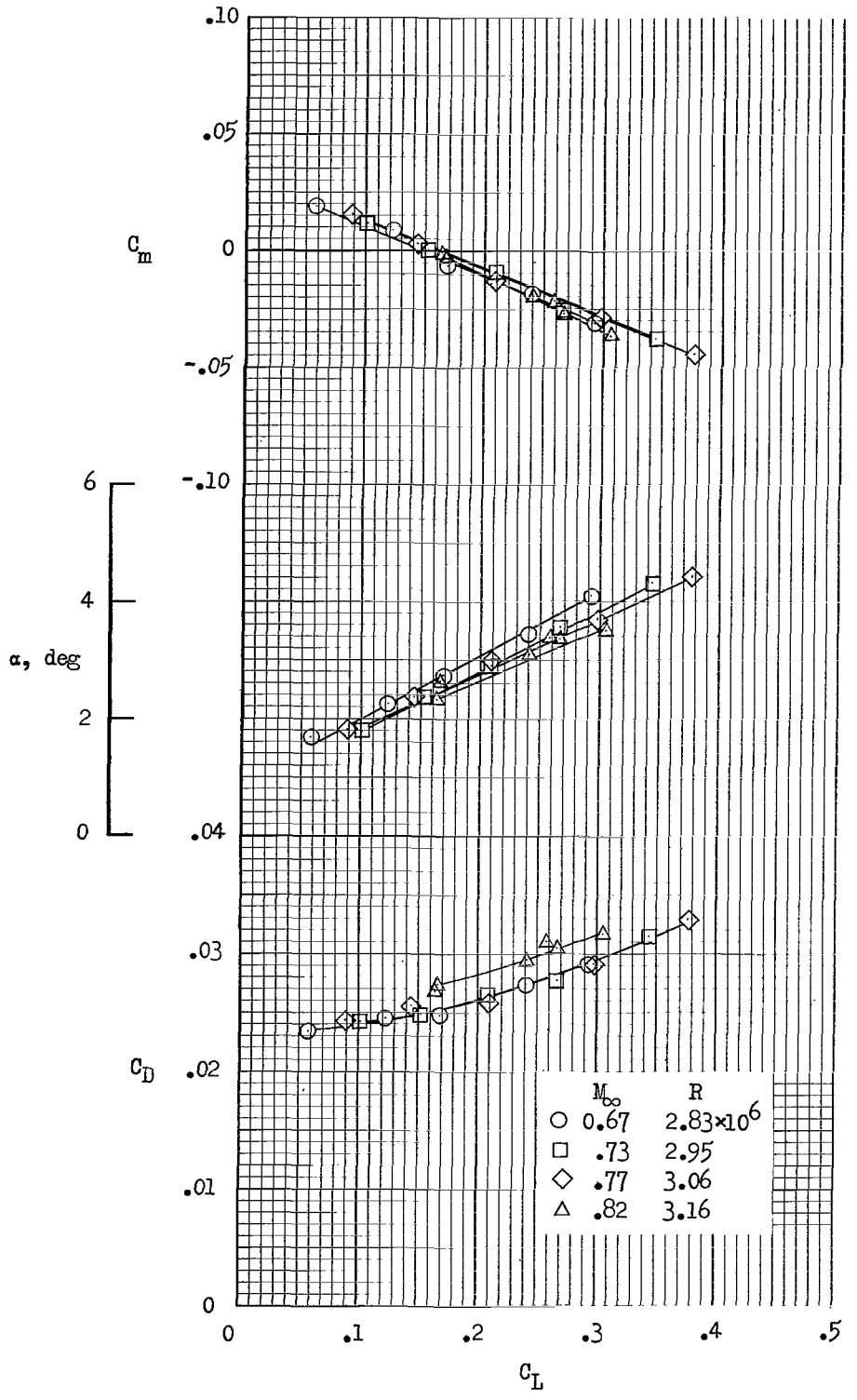

Figure 10.- Longitudinal aerodynamic characteristics of configuration BWVHN$_1$P$_1$ with $\delta_s = -0.80^0$, $i_n = 2.35^0$, $\Delta x/\bar{c} = 0$, and $\varepsilon = 0^0$.

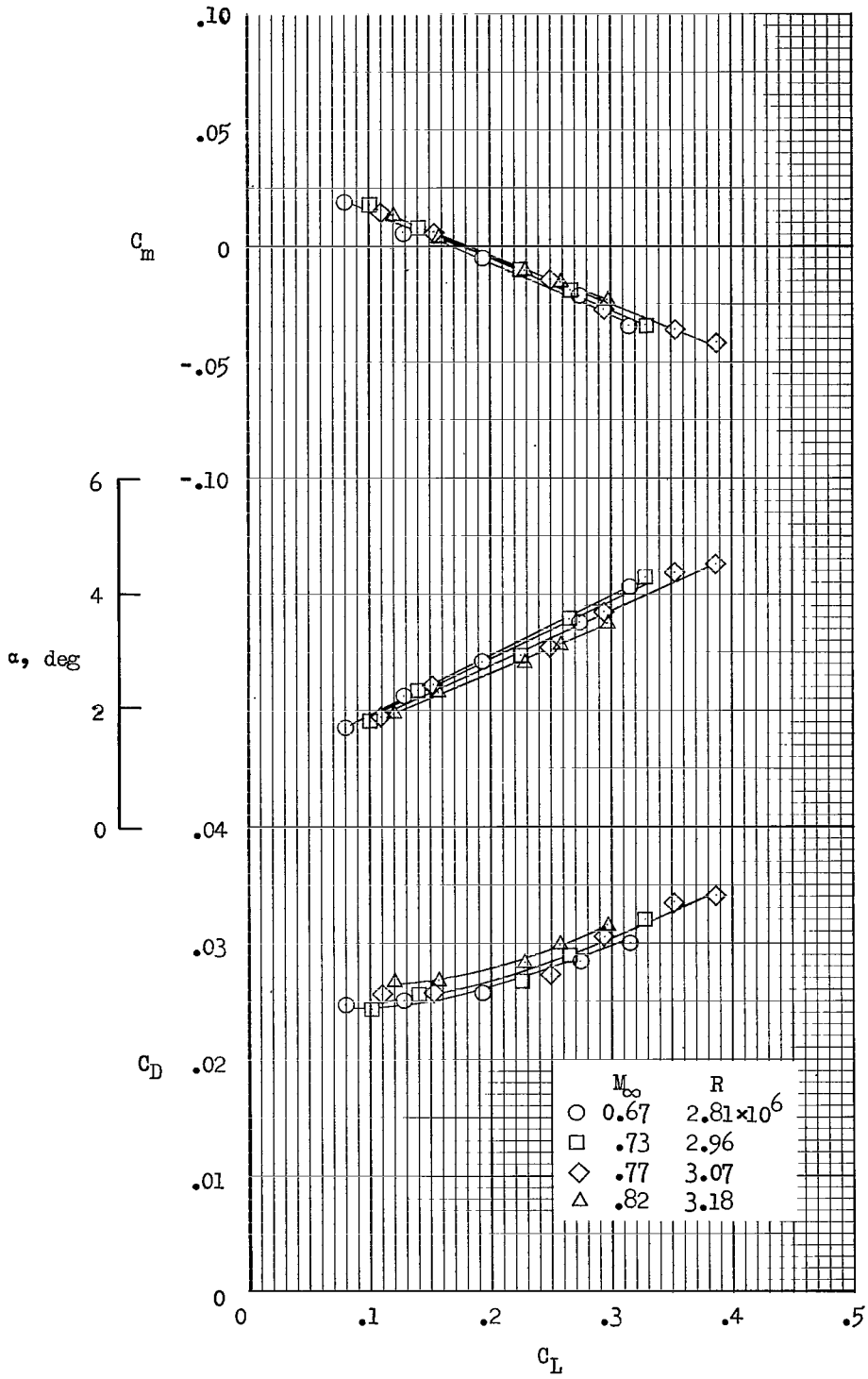

Figure 11.- Longitudinal aerodynamic characteristics of configuration $BWVHN_1P_1$ with $\delta_s = -0.80^0$, $i_n = 3.81^0$, $\Delta x/\bar{c} = 0$, and $\varepsilon = 0^0$.

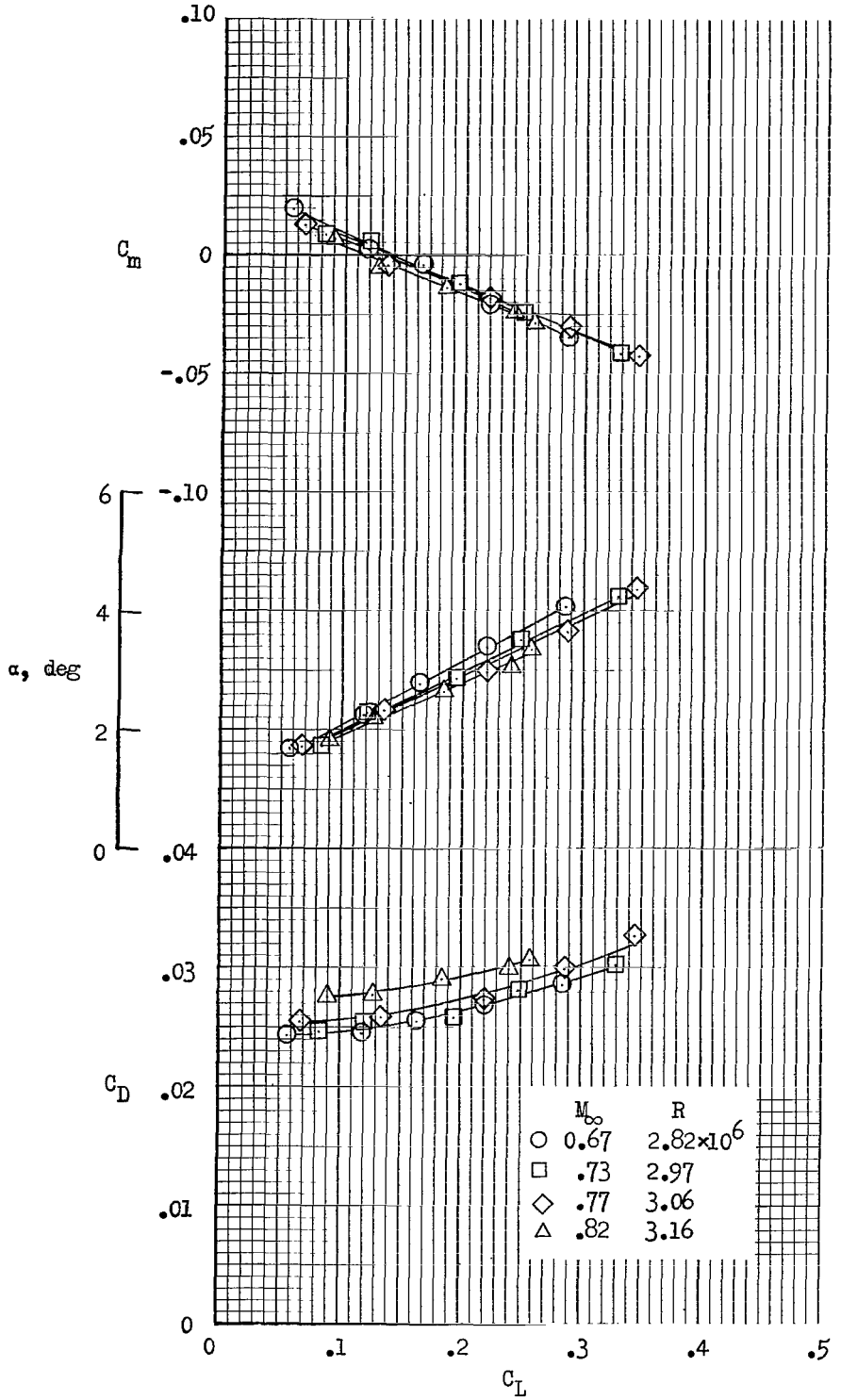

Figure 12.- Longitudinal aerodynamic characteristics of configuration BWVHN$_1$P$_1$ with $\delta_s = -0.80^0$, $i_n = 0.04^0$, $\Delta x/\bar{c} = -0.034$, and $\varepsilon = 0^0$.

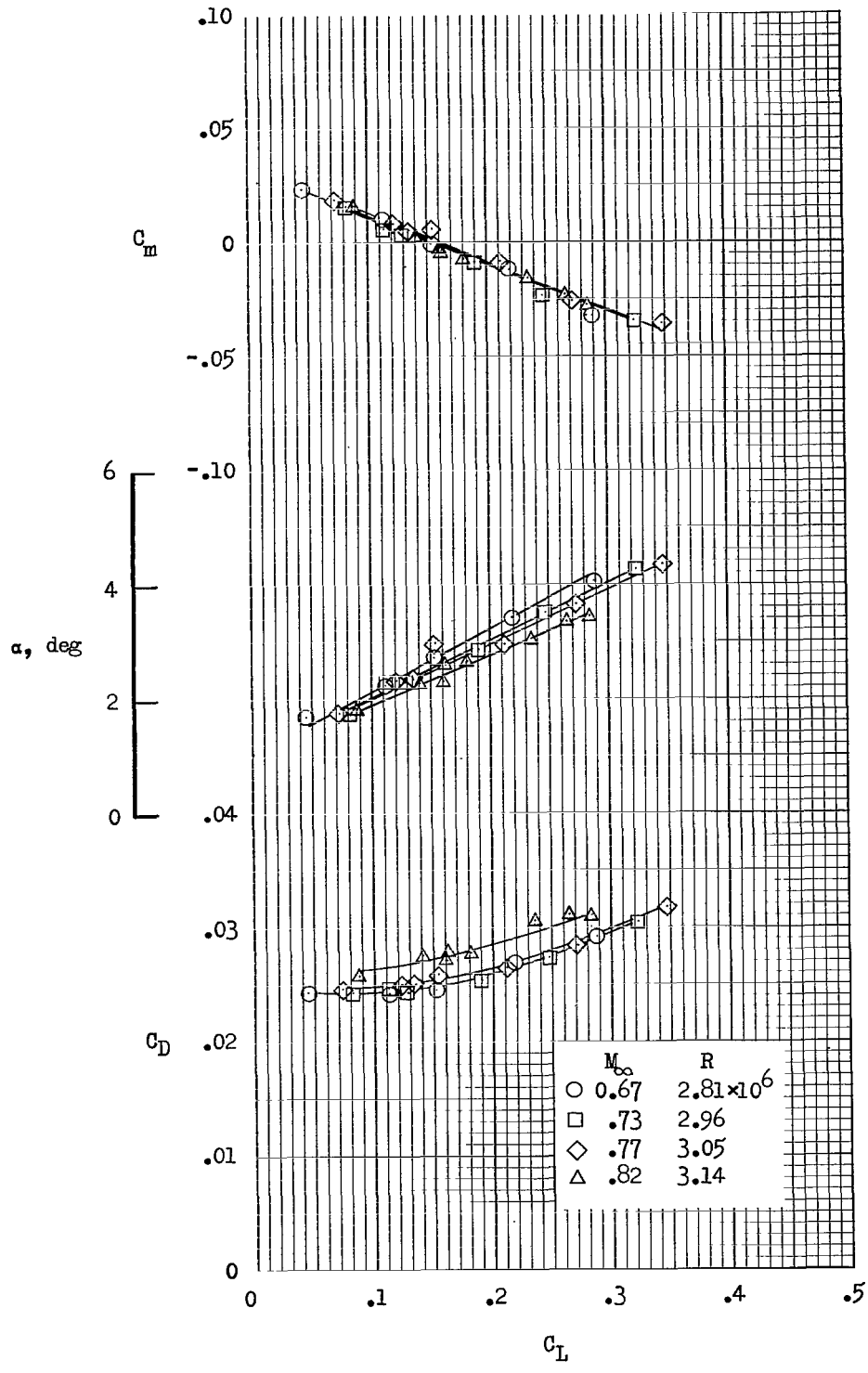

Figure 13.- Longitudinal aerodynamic characteristics of configuration BWVHN1P1 with $\delta_s = -0.80^0$, $i_n = 0.06^0$, $\Delta x/\bar{c} = 0.072$, and $\epsilon = 0^0$.

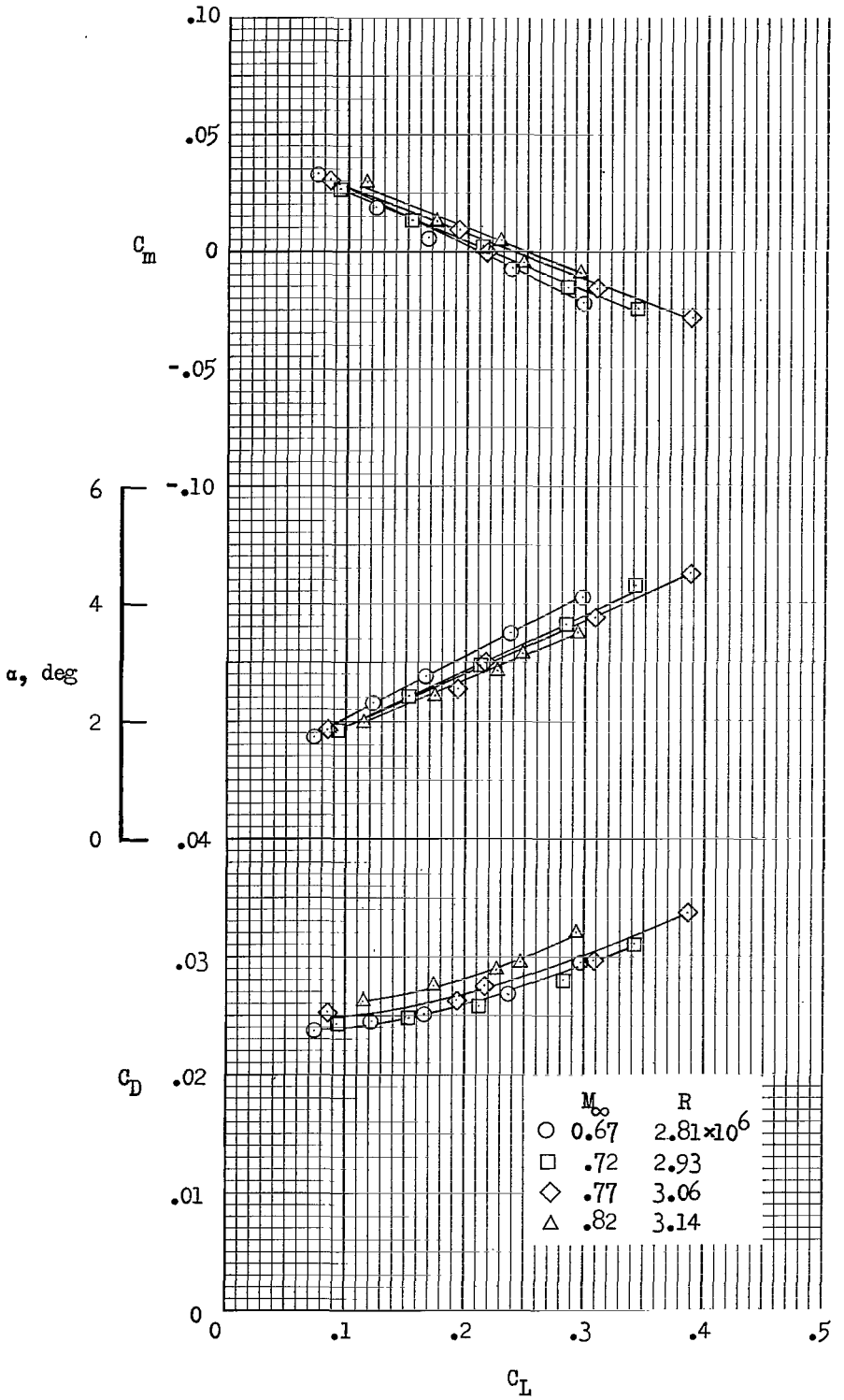

Figure 14.- Longitudinal aerodynamic characteristics of configuration $BWVHN_1P_1$ with $\delta_s = -0.80^0$, $i_n = 0.14^0$, $\Delta x/\bar{c} = 0.237$, and $\varepsilon = 0^0$.

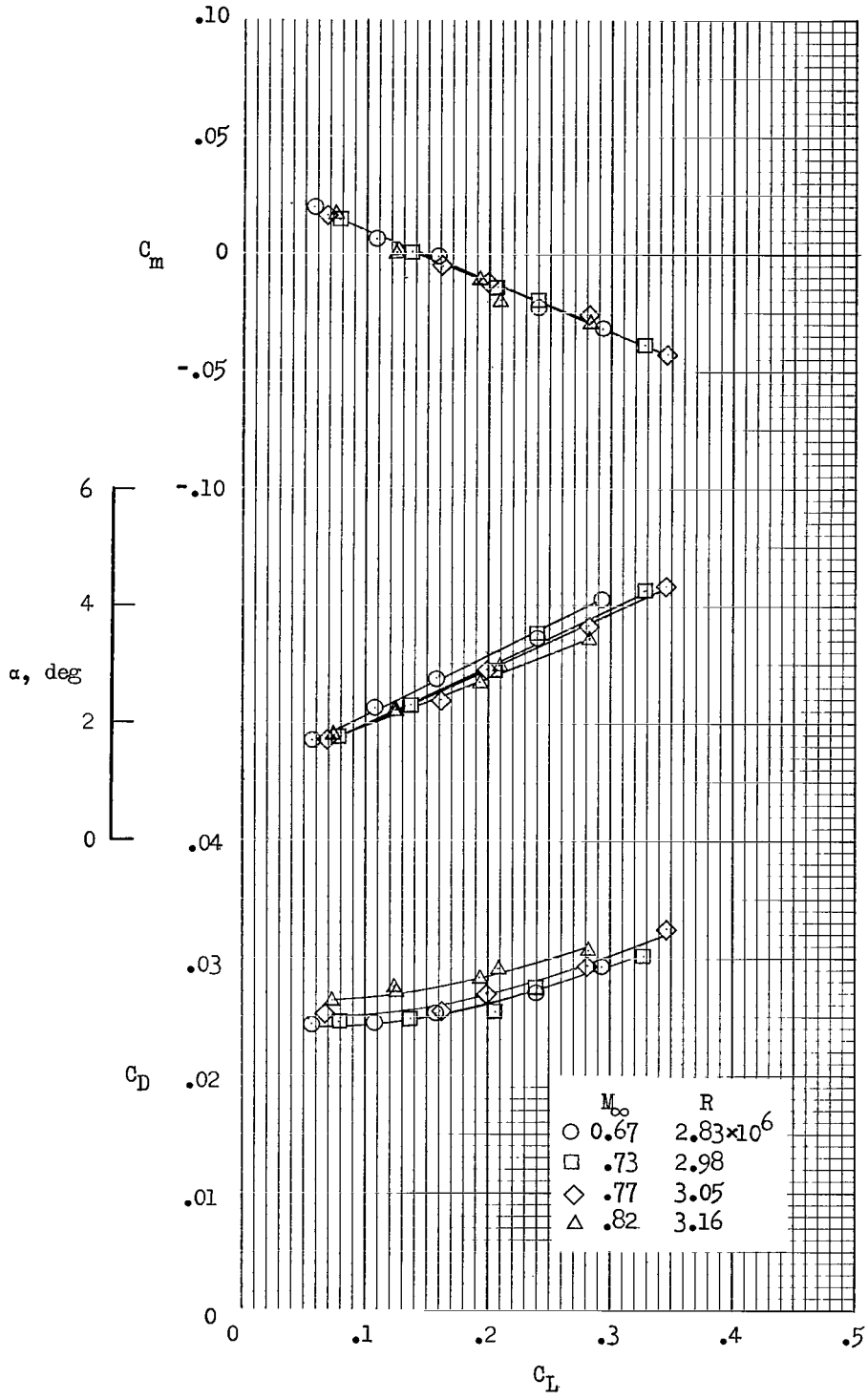

Figure 15.- Longitudinal aerodynamic characteristics of configuration $BWVHN_1P_1$ with $\delta_s = -0.80^o$, $i_n = -0.04^o$, $\Delta x/\bar{c} = 0$, and $\varepsilon = 3.5^o$.

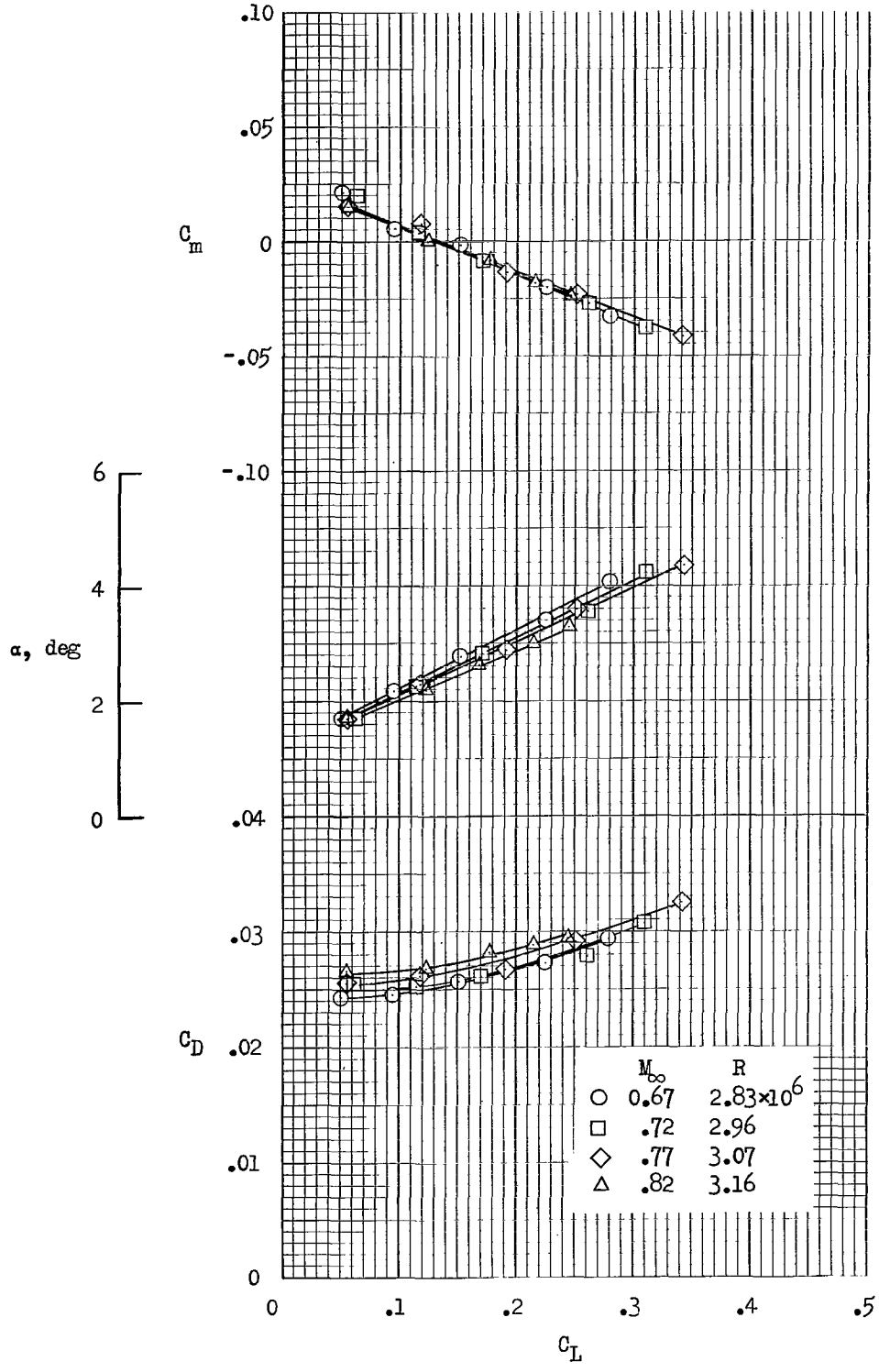

Figure 16.- Longitudinal aerodynamic characteristics of configuration BWVHN$_2$P$_1$ with $\delta_s = -0.80^0$, $i_n = -0.02^0$, $\Delta x/\bar{c} = 0$, and $\varepsilon = 0^0$.

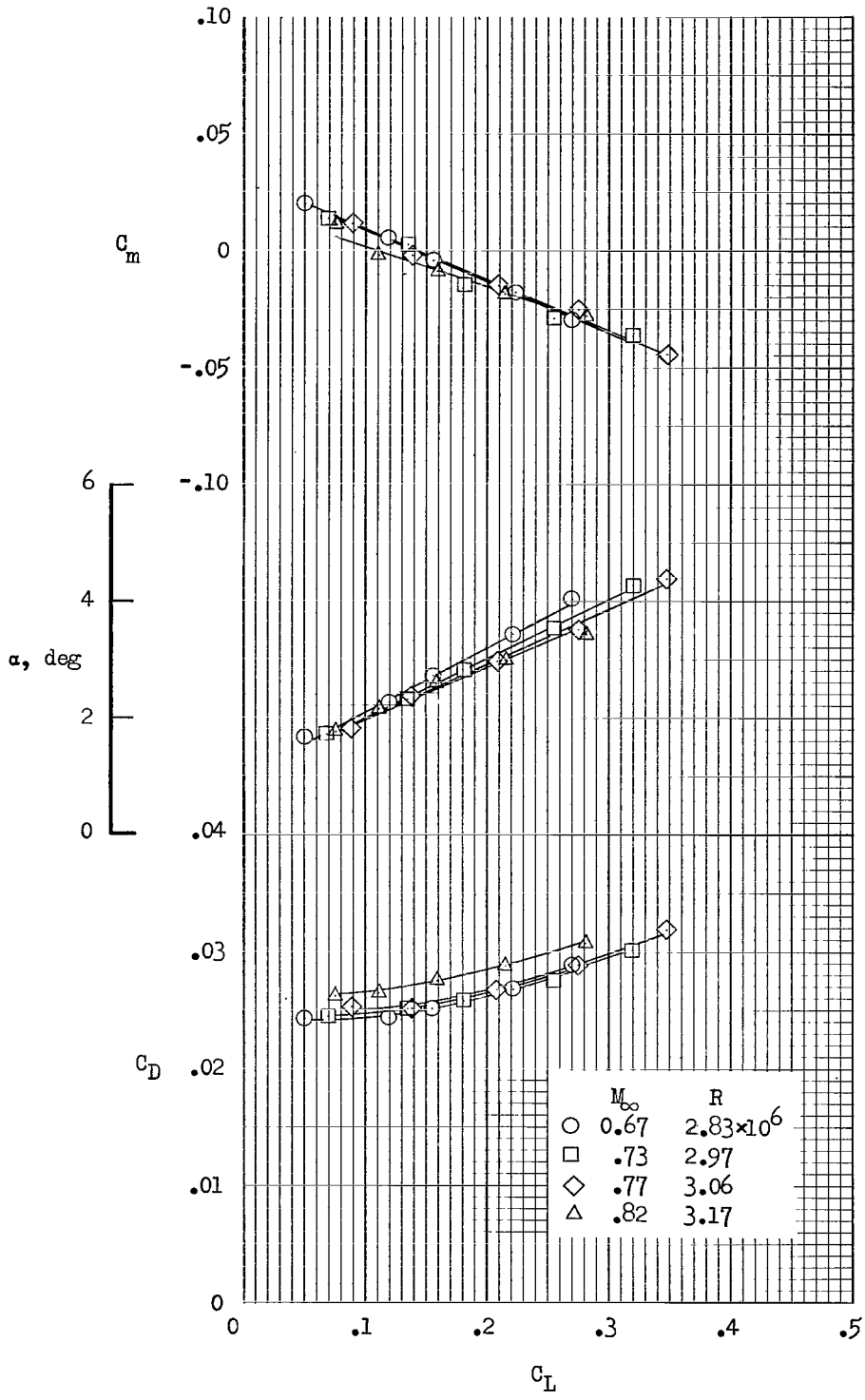

Figure 17.- Longitudinal aerodynamic characteristics of configuration BWVHN$_2$P$_2$ with $\delta_s = -0.80^0$, $i_n = -0.02^0$, $\Delta x/\bar{c} = 0$, and $\varepsilon = 0^0$.

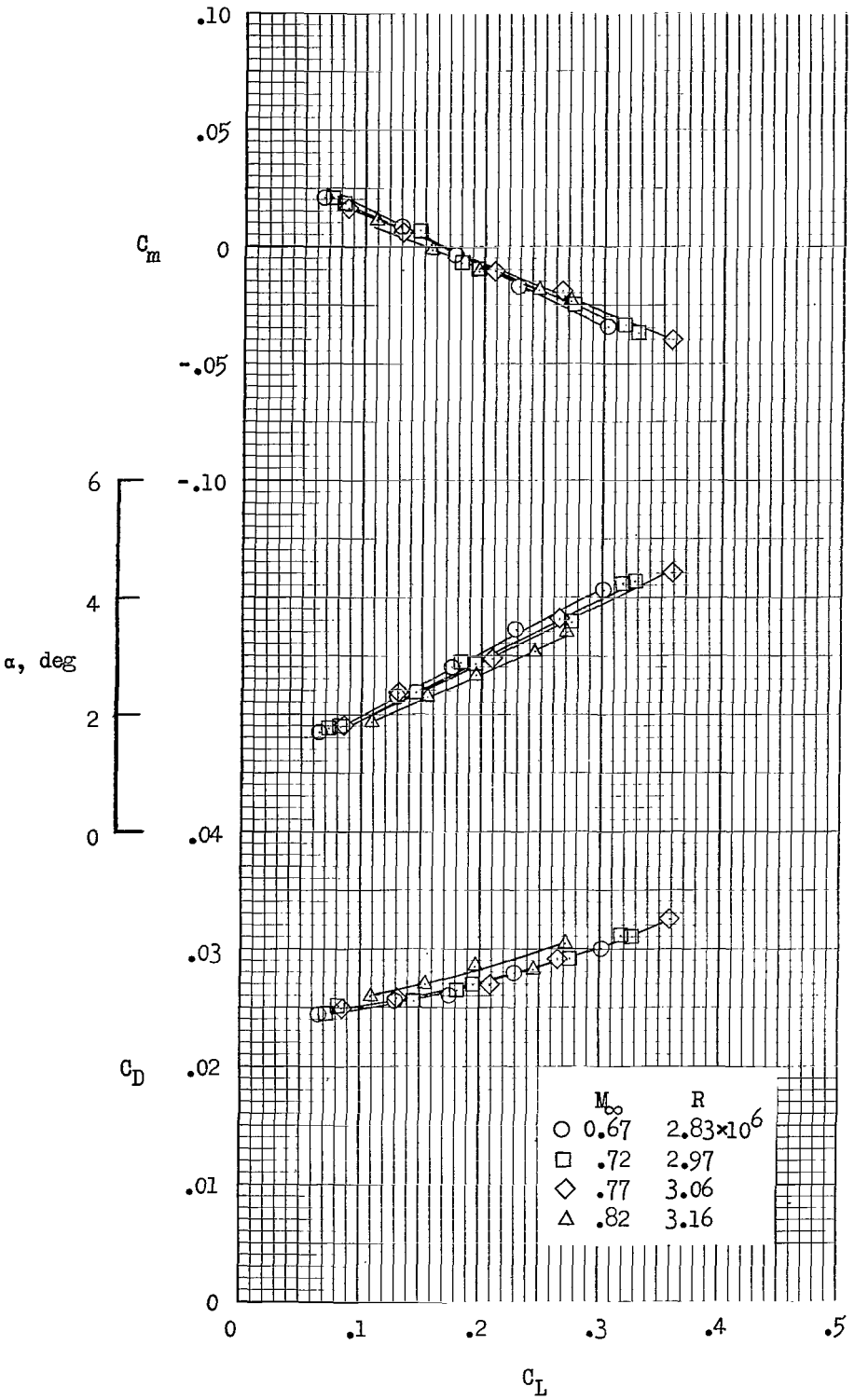

Figure 18.- Longitudinal aerodynamic characteristics of configuration BWVHN$_2$P$_1$ with $\delta_s = -0.80^0$, $i_n = 1.85^0$, $\Delta x/\bar{c} = 0$, and $\varepsilon = 0^0$.

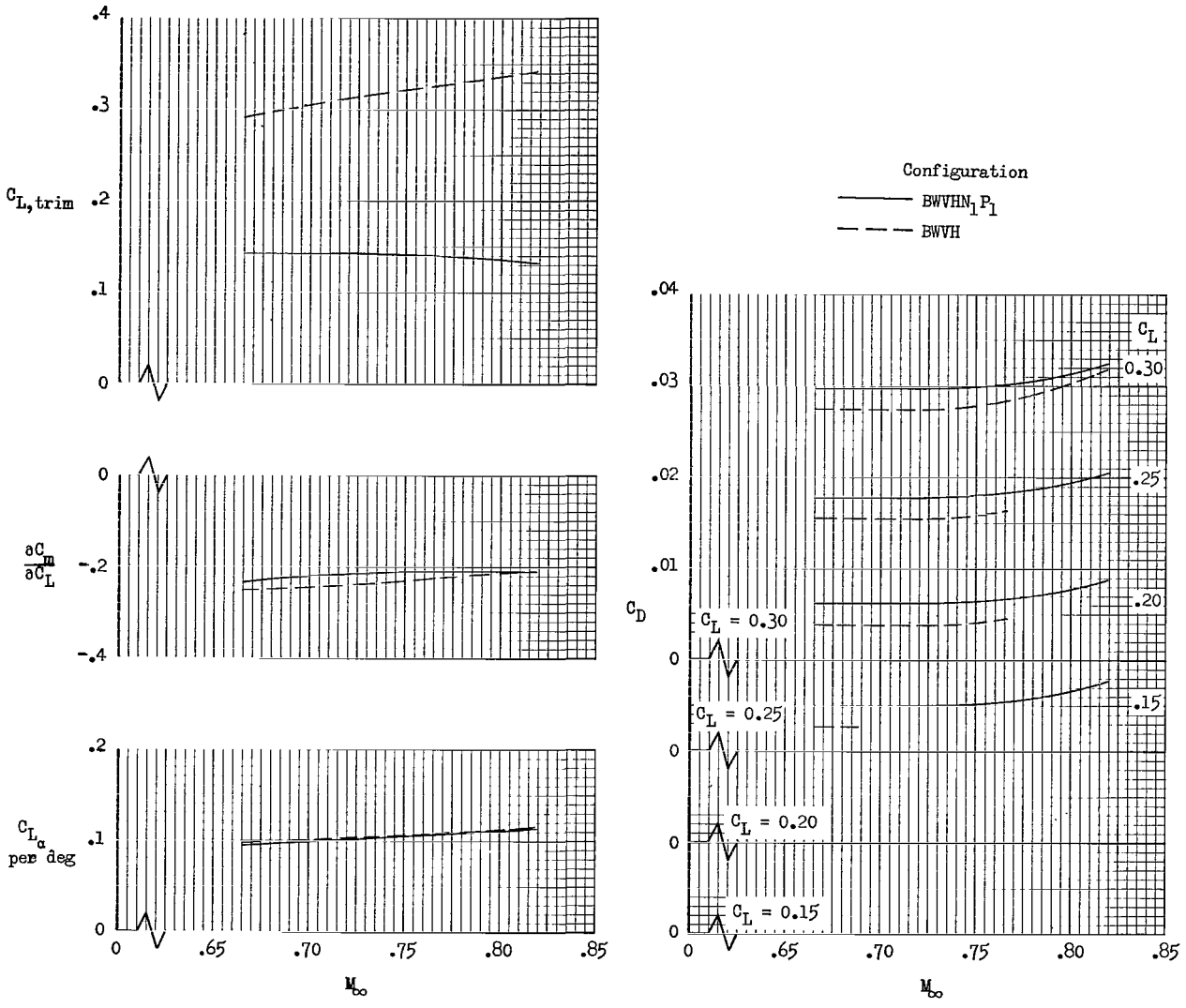

Figure 19.- Effects of nacelles and pylons on the aerodynamic characteristics of the model with $\delta_s = -0.80^0$.

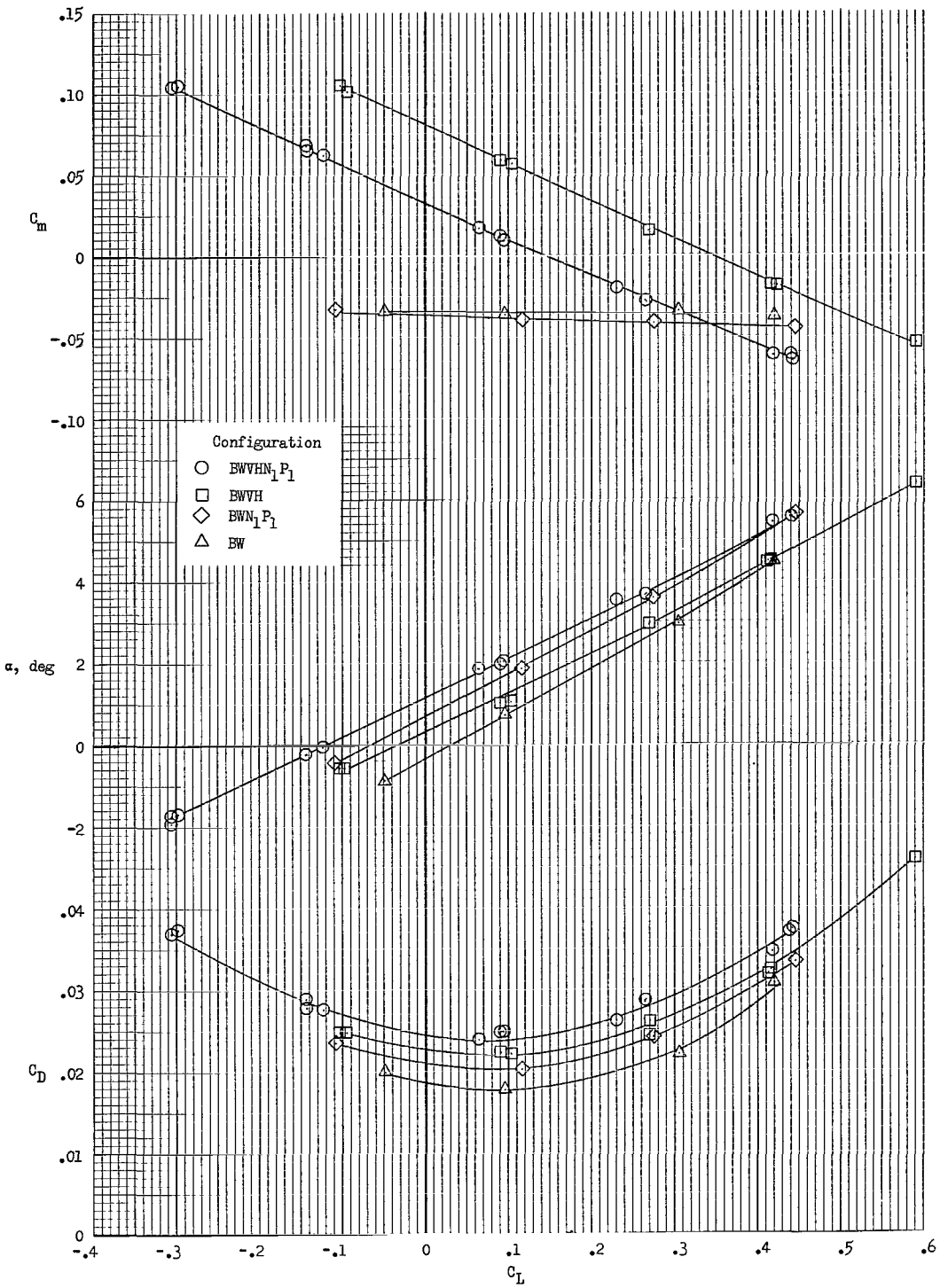

Figure 20.- Effects of addition of vertical tail and horizontal tail at $\delta_s = -0.80^0$ and nacelles at $i_n \approx 0^0$, $\Delta x/\bar{c} = 0$, and $\varepsilon = 0^0$ on the longitudinal aerodynamic characteristics of the model. $M_\infty = 0.72$; $R = 3.69 \times 10^6$.

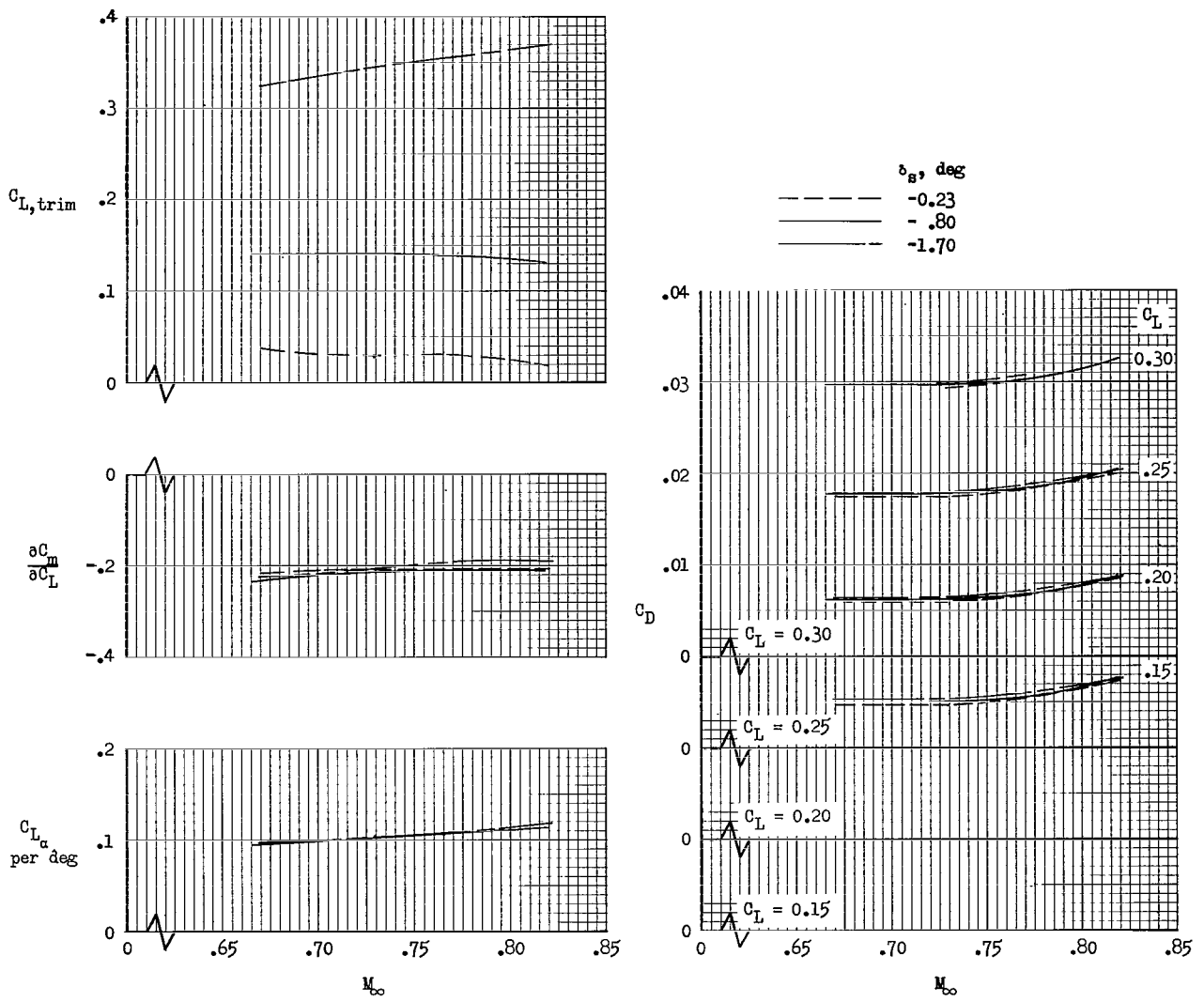

(a) Variation of $C_{L,trim}$, $\partial C_m/\partial C_L$, C_{L_α}, and C_D with M_∞.

Figure 21.- Effects of horizontal-stabilizer deflection angle on the aerodynamic characteristics of configuration BWVHN$_1$P$_1$ with $i_n = 0.06^0$, $\Delta x/\bar{c} = 0$, and $\varepsilon = 0^0$.

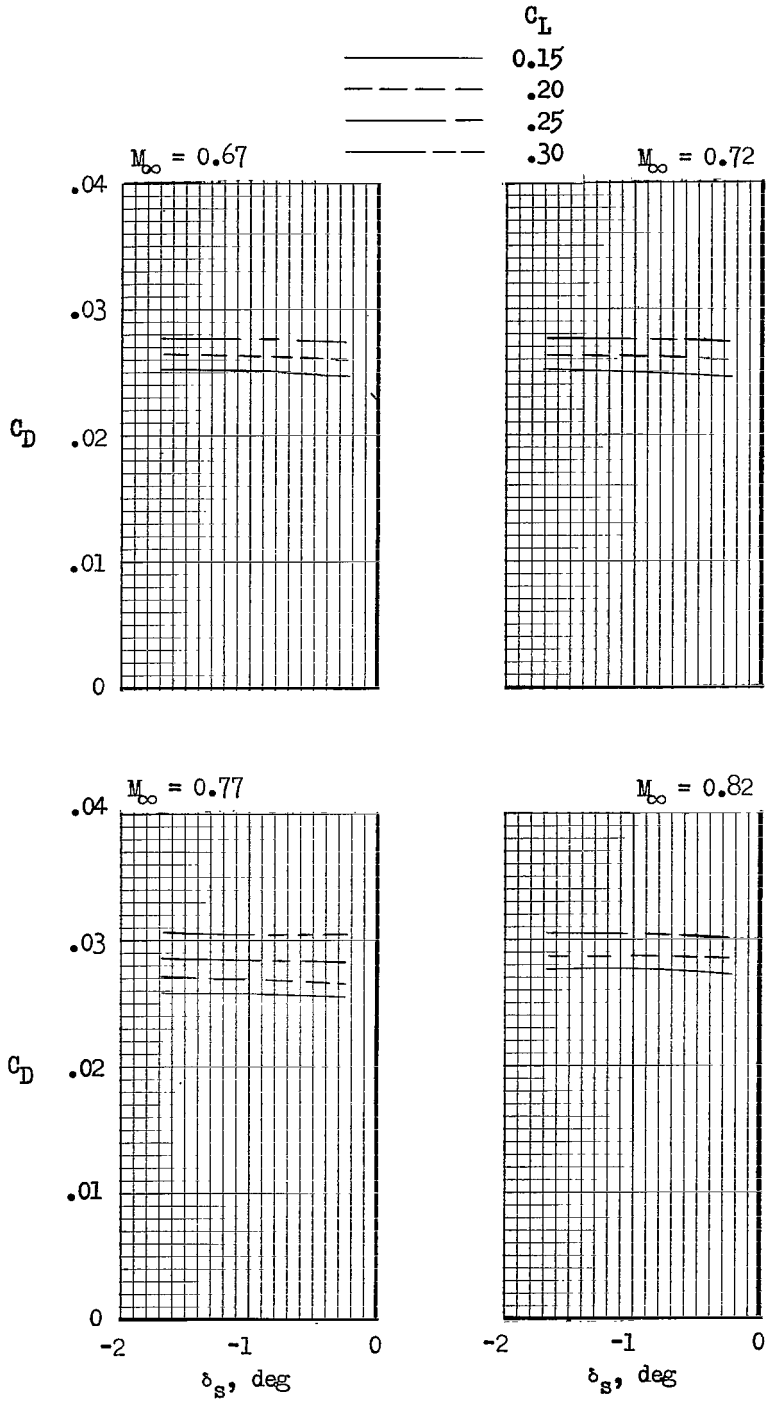

(b) Variation of C_D with δ_s.

Figure 21.- Concluded.

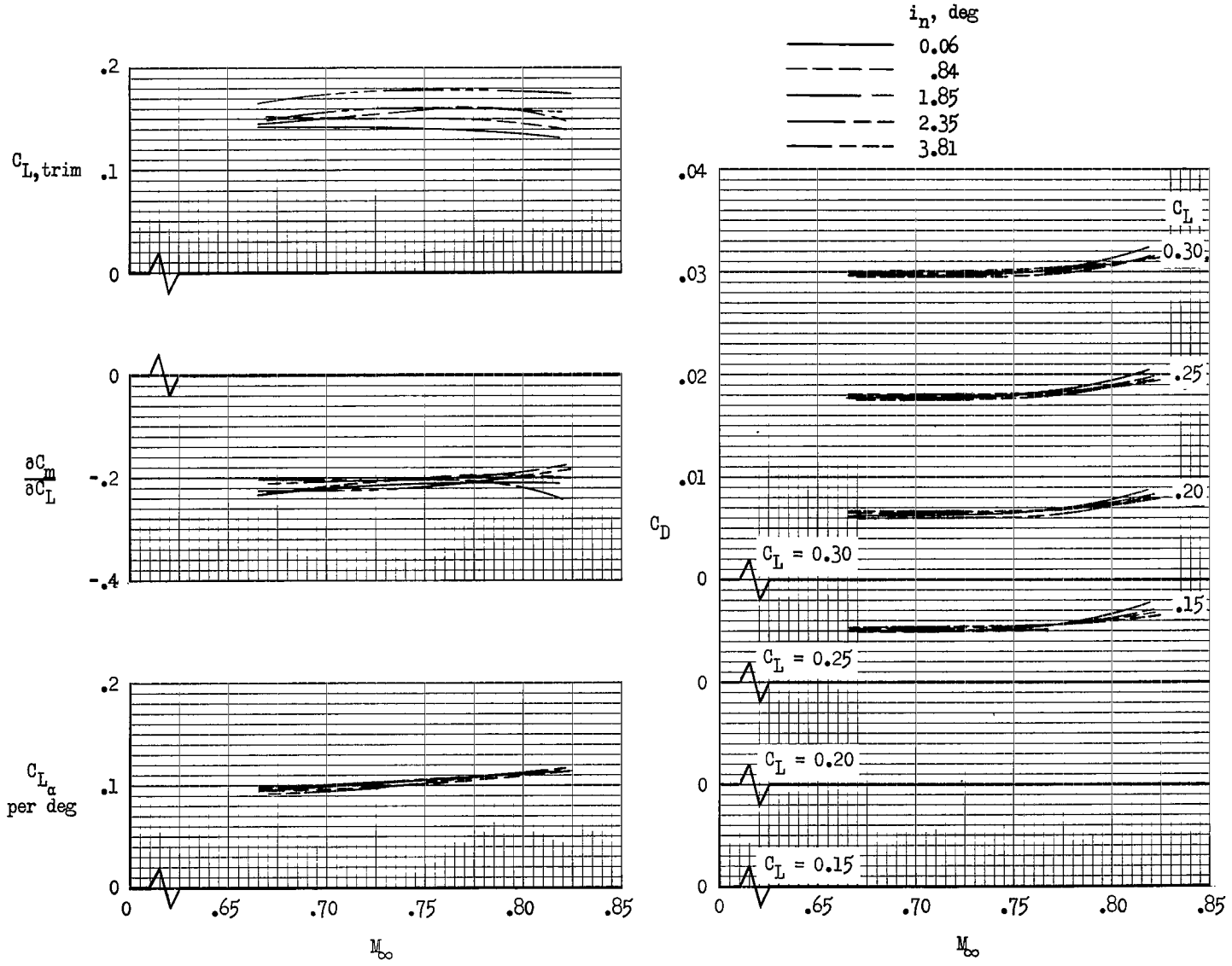

(a) Variation of $C_{L,trim}$, $\partial C_m/\partial C_L$, C_{L_α}, and C_D with M_∞.

Figure 22.- Effects of nacelle incidence on the aerodynamic characteristics of configuration BWVHN1P1 with $\delta_s = -0.80^0$, $\Delta x/\bar{c} = 0$, and $\varepsilon = 0^0$.

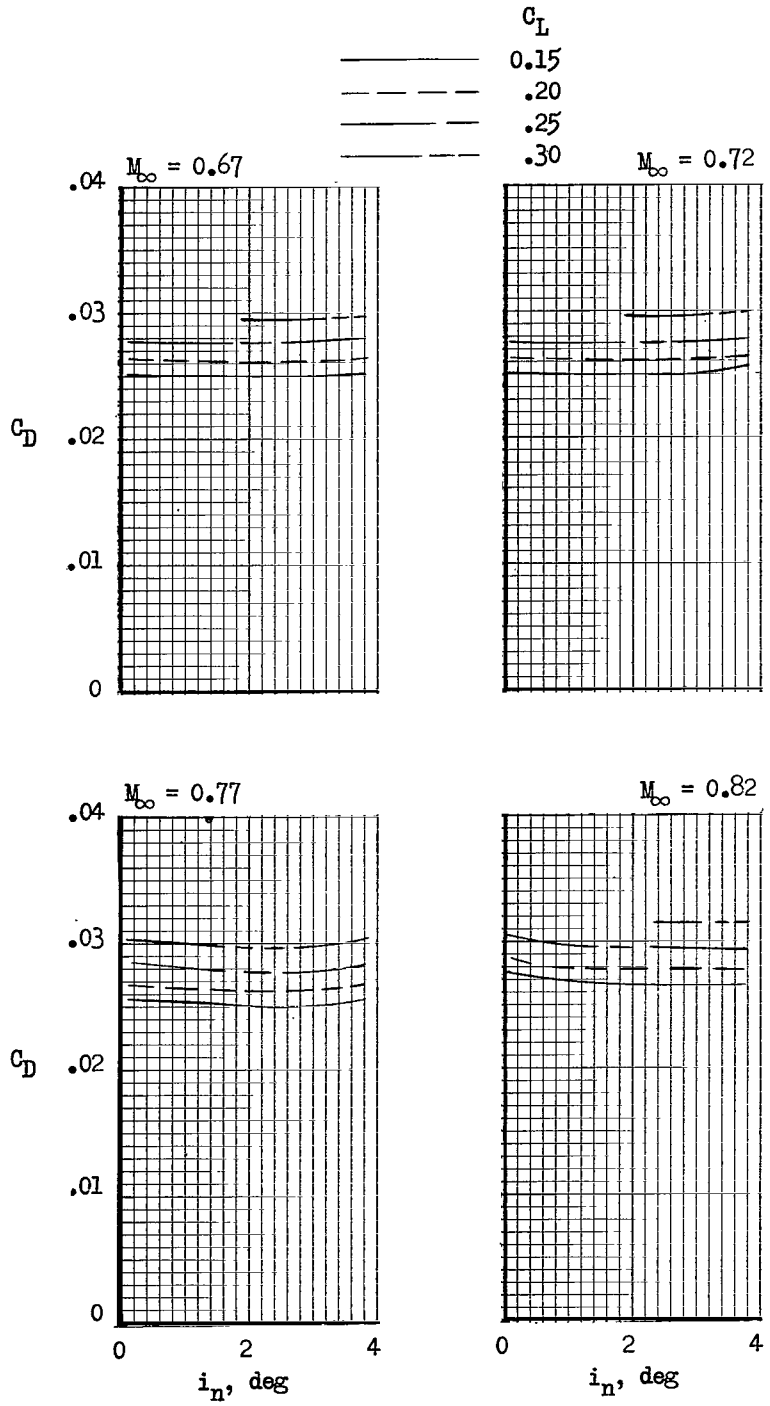

(b) Variation of C_D with i_n.

Figure 22.- Concluded.

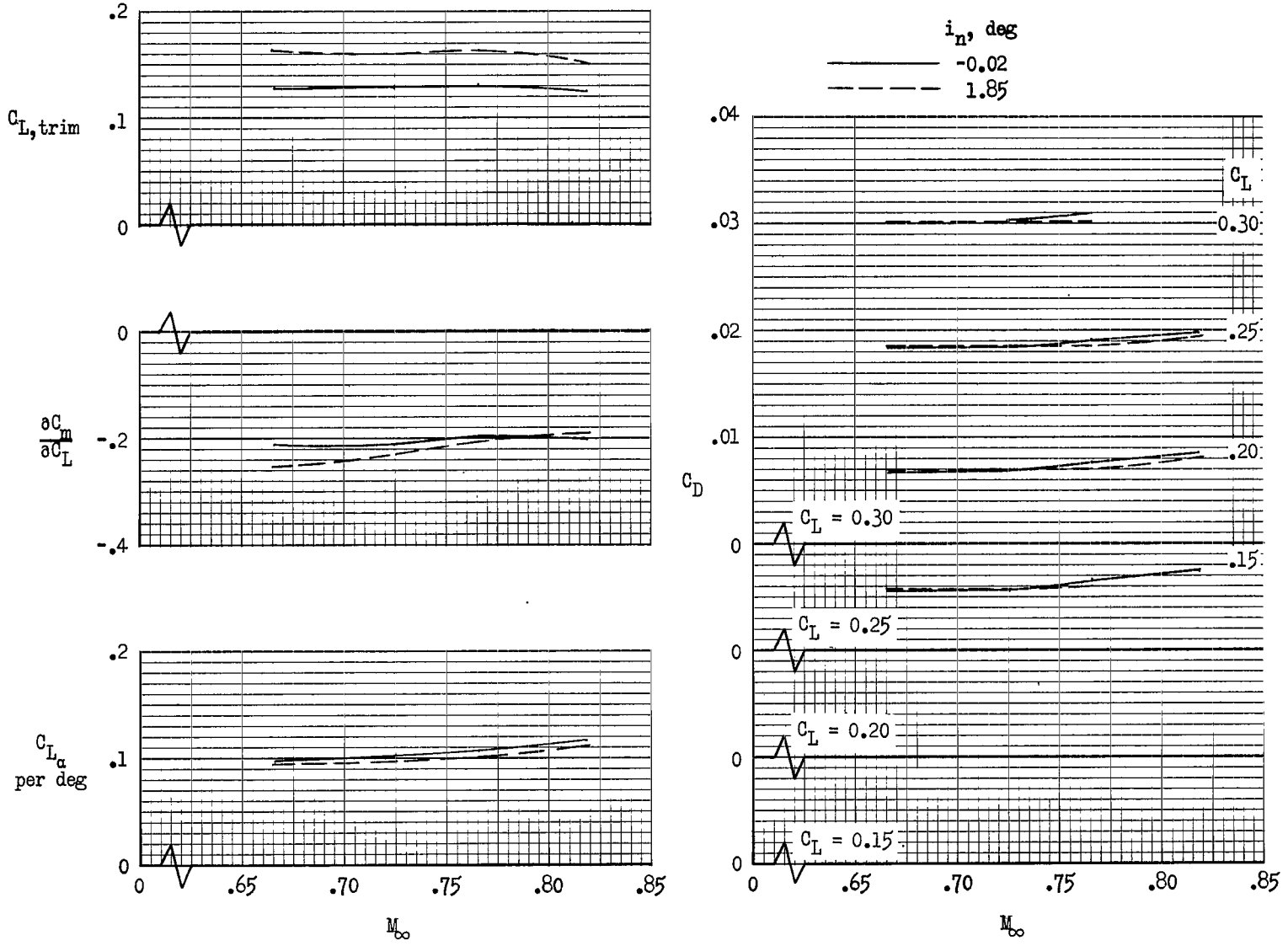

Figure 23.- Effects of nacelle incidence on the aerodynamic characteristics of configuration BWVHN$_2$P$_1$ with $\delta_s = -0.80^o$, $\Delta x/\bar{c} = 0$, and $\varepsilon = 0^o$.

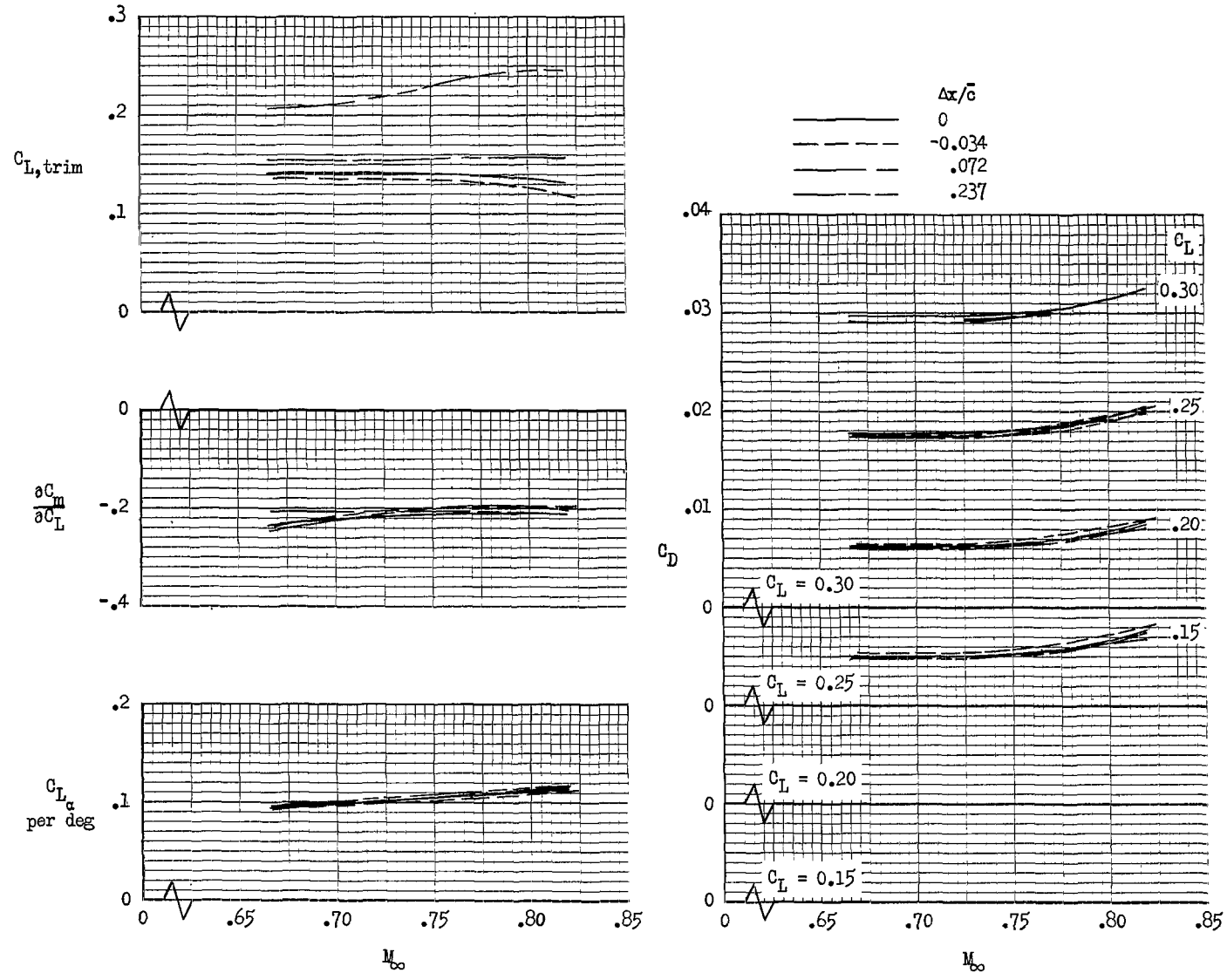

(a) Variation of $C_{L,trim}$, $\partial C_m/\partial C_L$, C_{L_α}, and C_D with M_∞.

Figure 24.- Effects of nacelle longitudinal location on the aerodynamic characteristics of configuration BWVHN$_1$P$_1$ with $\delta_s = -0.80^0$, $i_n \approx 0^0$, and $\varepsilon = 0^0$.

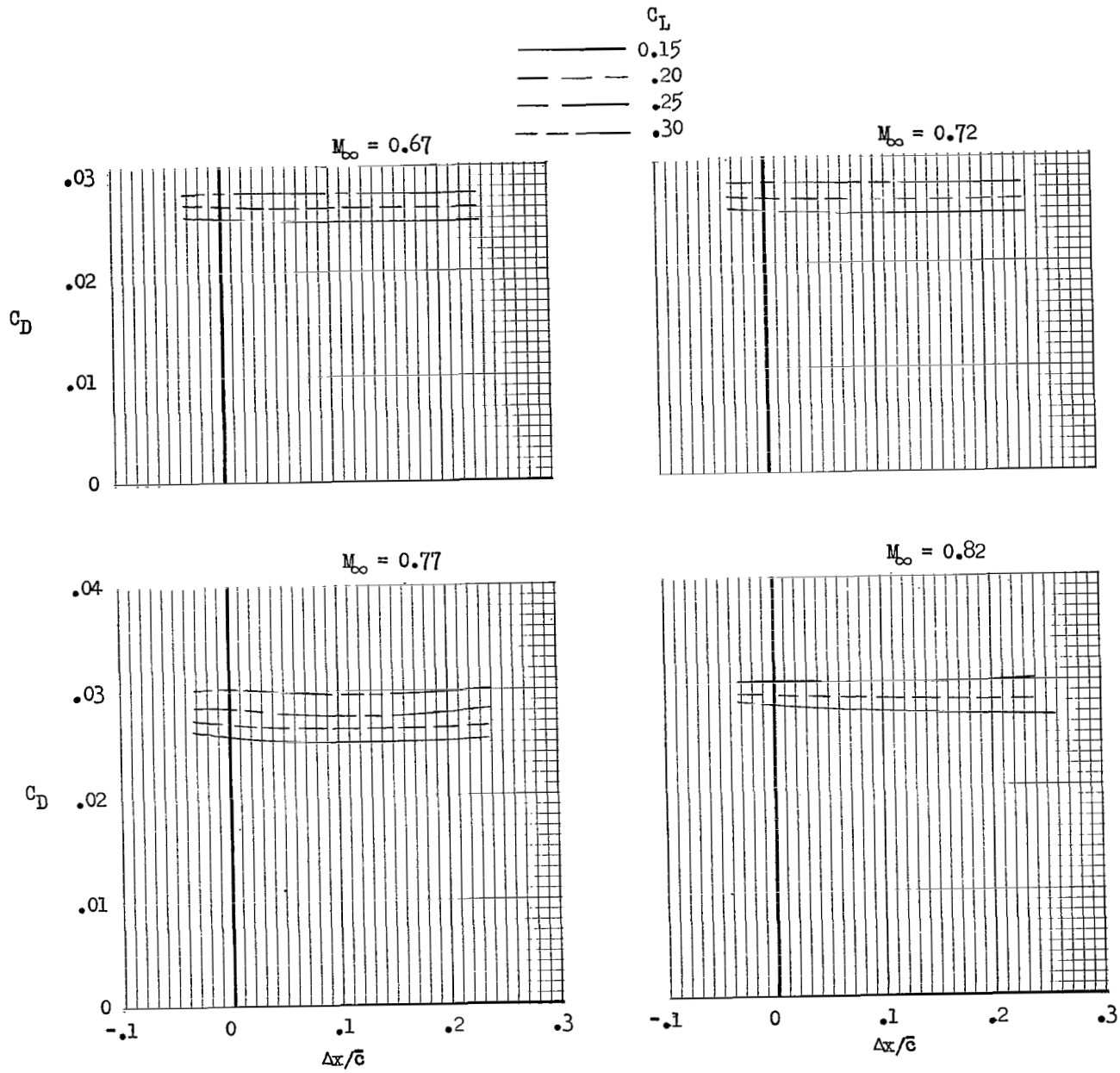

(b) Variation of C_D with $\Delta x/\bar{c}$.

Figure 24.- Concluded.

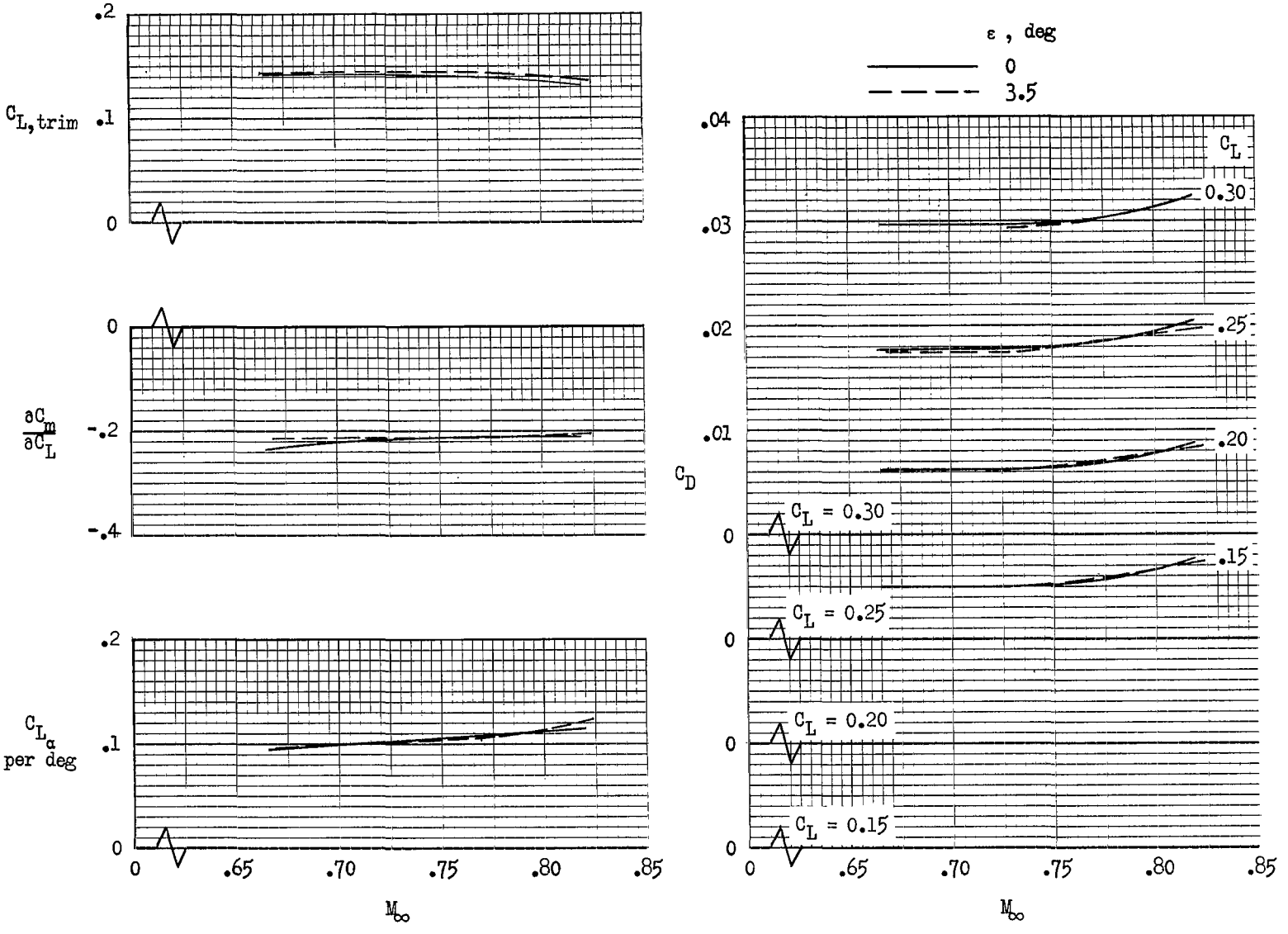

Figure 25.- Effects of nacelle cant (yaw) on the aerodynamic characteristics of configuration BWVHN$_1$P$_1$ with $\delta_s = -0.80^0$, $i_n \approx 0^0$, and $\Delta x/\bar{c} = 0$.

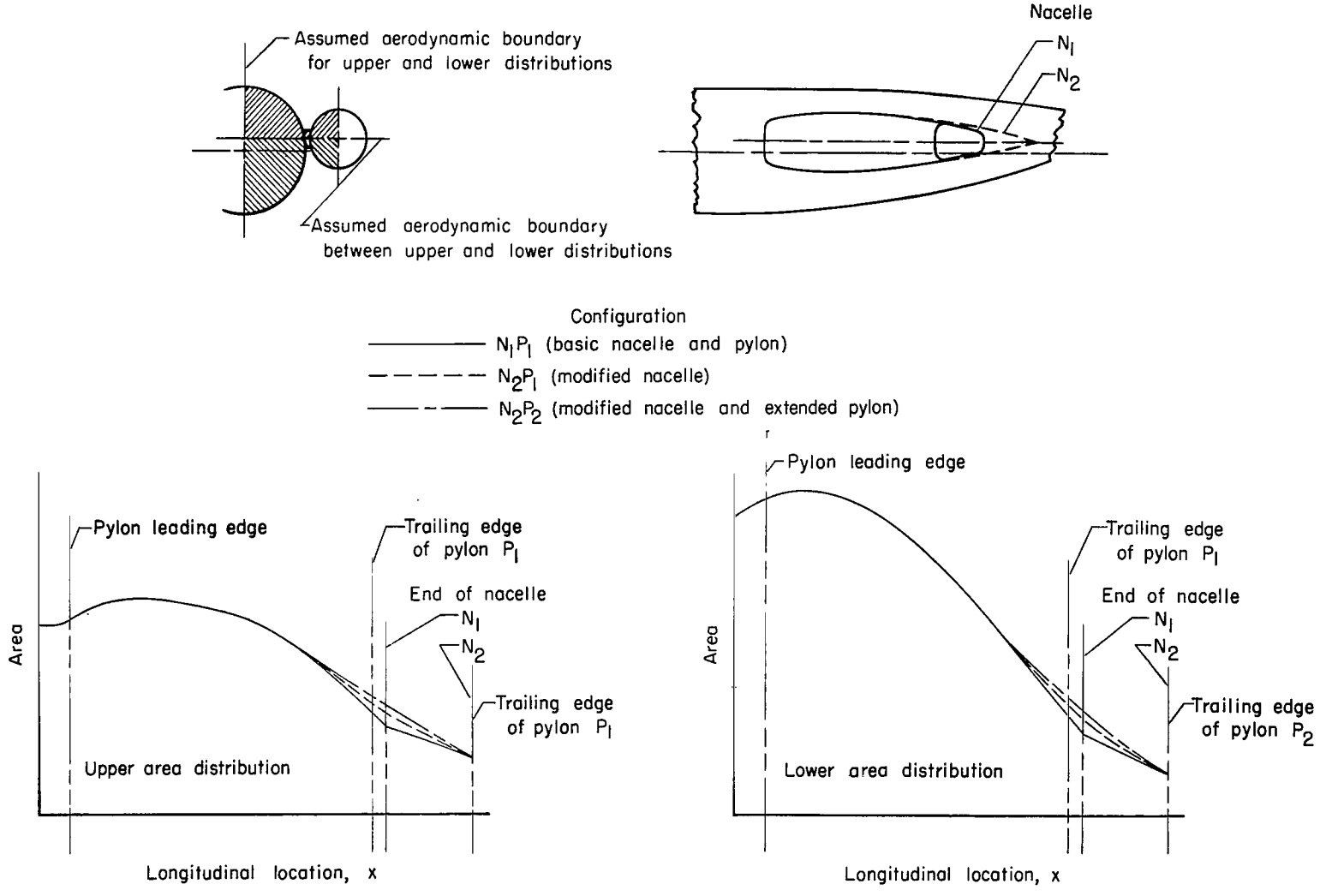

Figure 26.- Local area distributions.

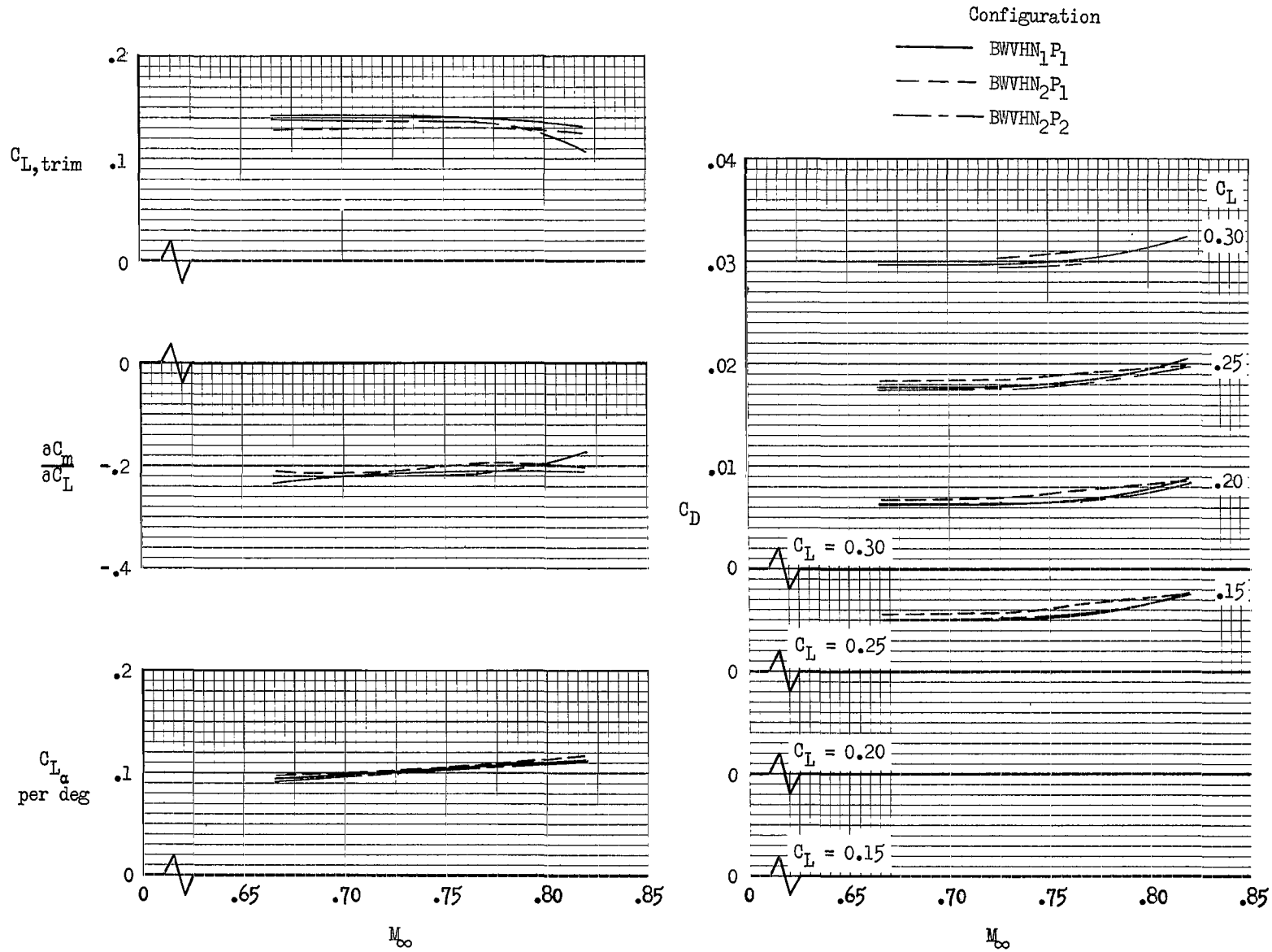

Figure 27.- Effects of nacelle shape and pylon extensions on the aerodynamic characteristics of the model with $\delta_s = -0.80^0$, $i_n \approx 0^0$, $\Delta x/\bar{c} = 0$, and $\epsilon = 0^0$.

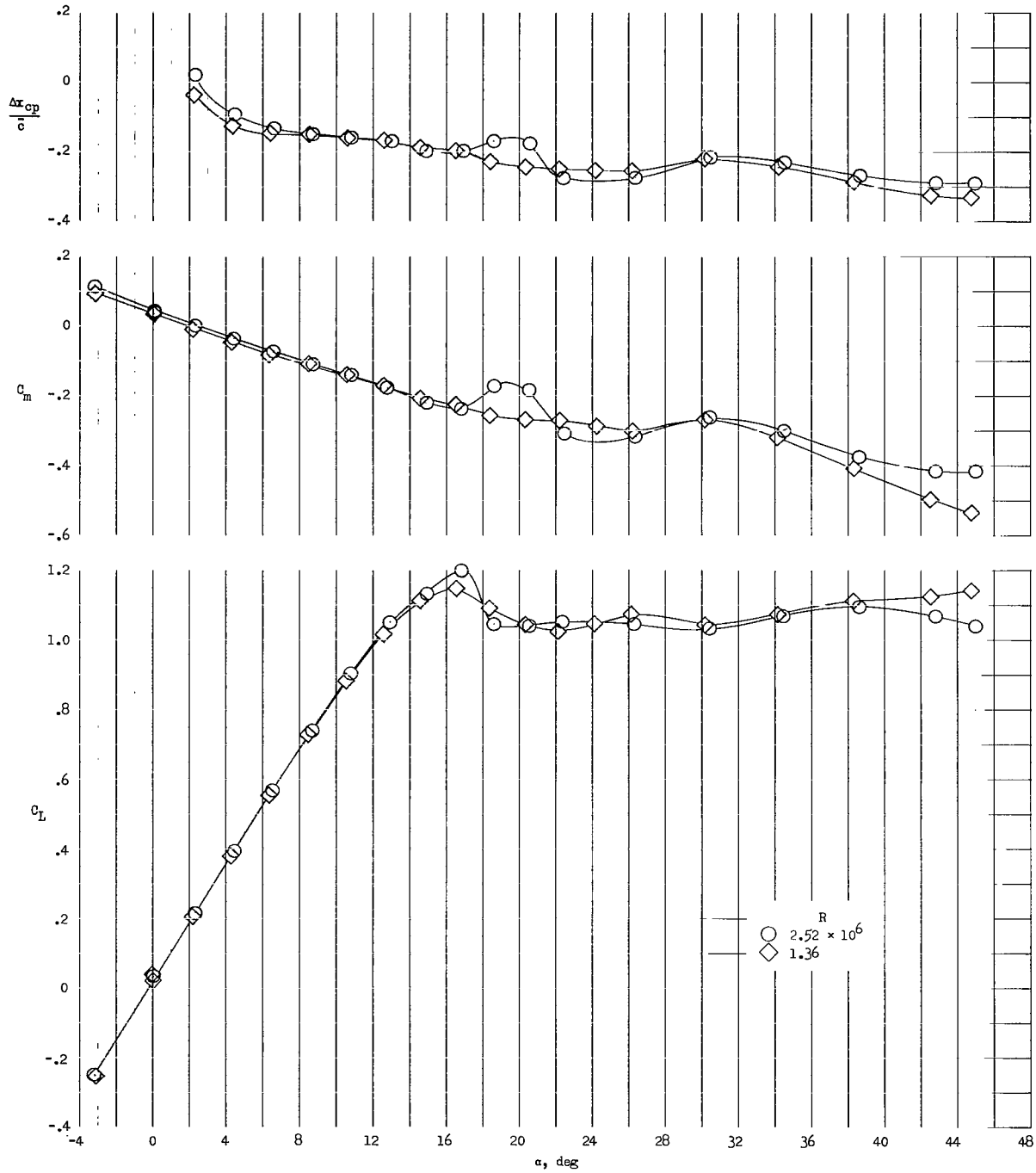

(a) Variation of C_L, C_m, and $\Delta x_{cp}/\bar{c}$ with α.

Figure 28.- Effects of Reynolds number on the longitudinal aerodynamic characteristics of configuration BWVH with $\delta_S = -0.23^0$. $M_\infty \approx 0.2$.

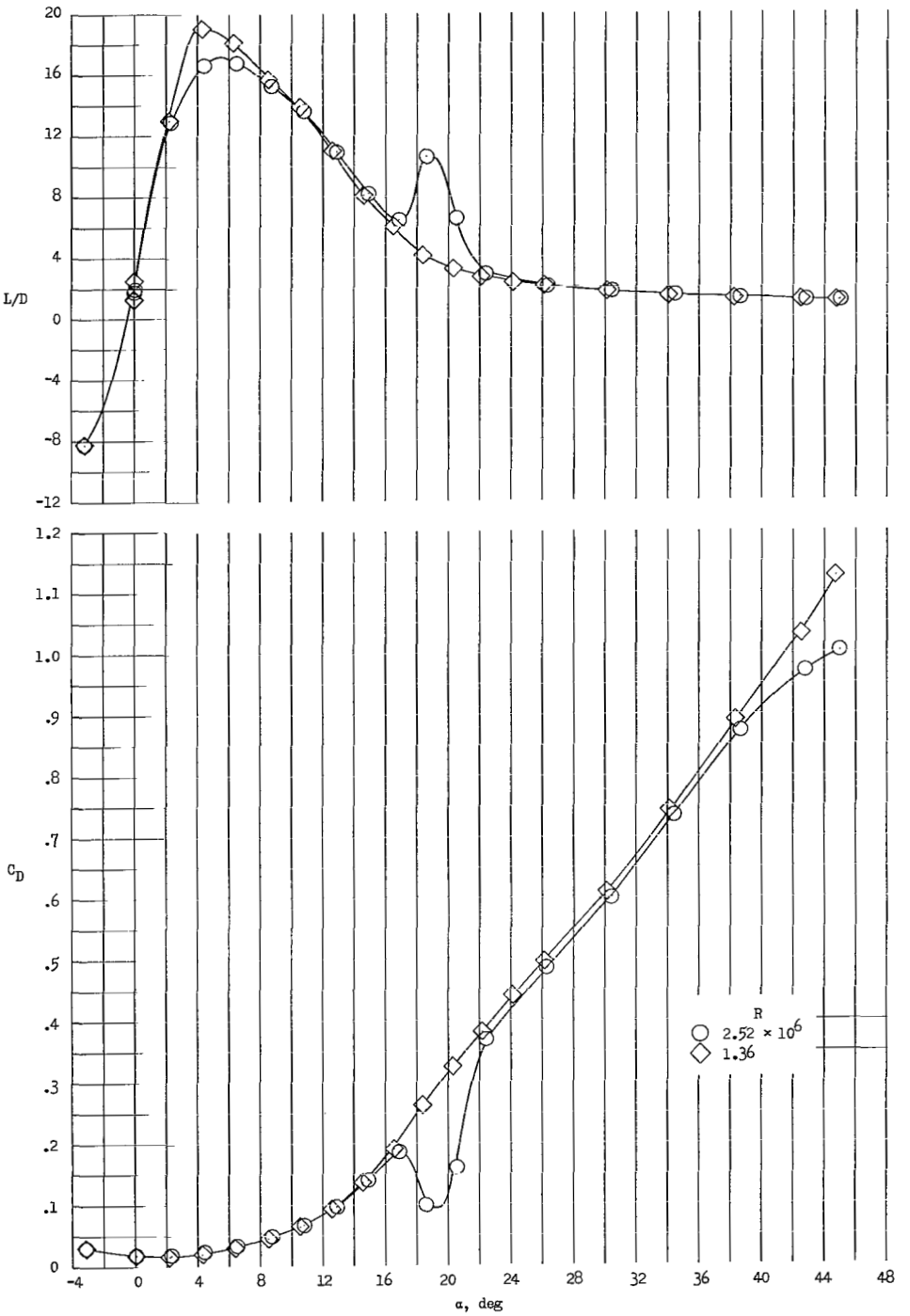

(b) Variation of C_D and L/D with α.

Figure 28.- Concluded.

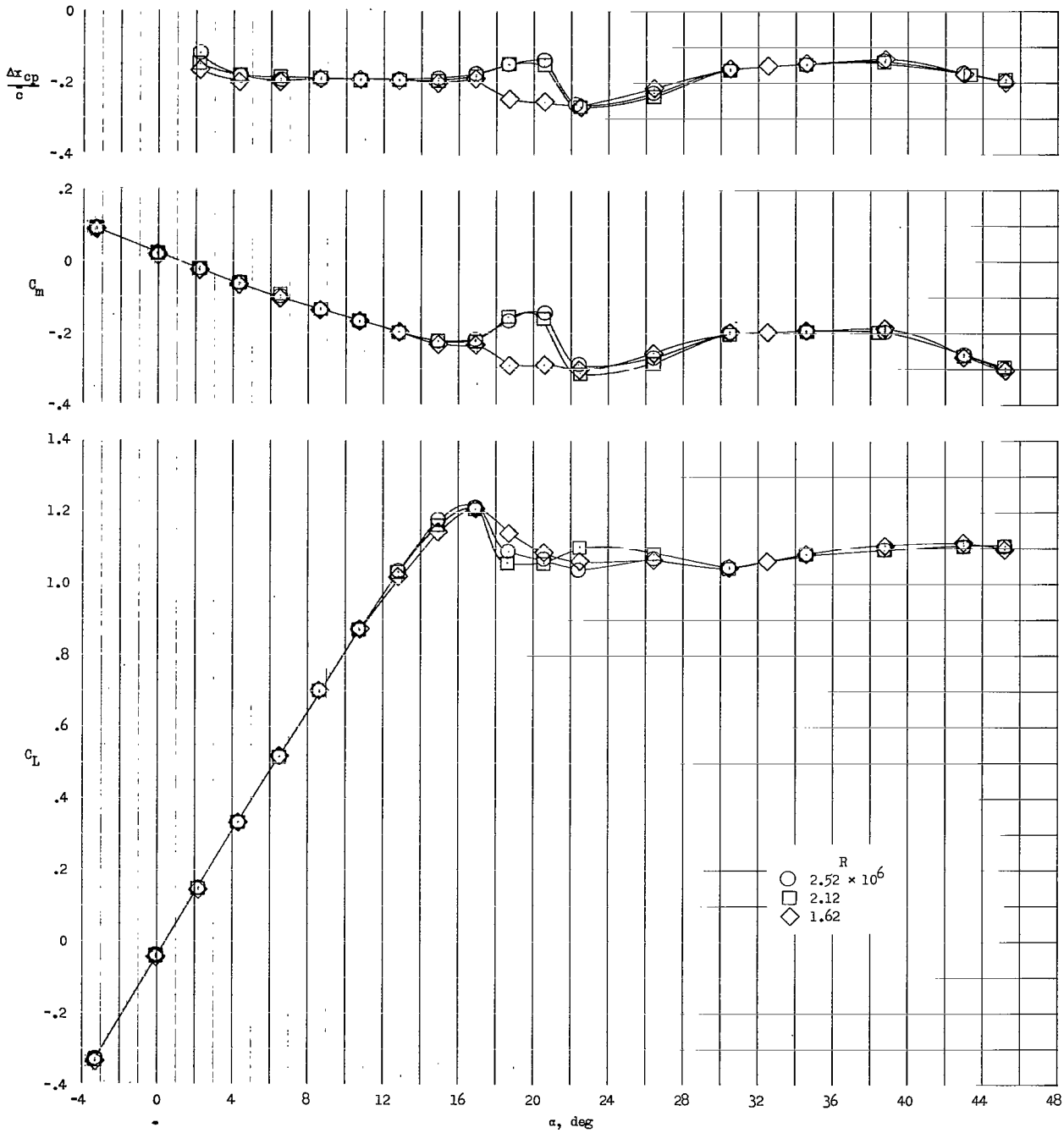

(a) Variation of C_L, C_m, and $\Delta x_{cp}/\bar{c}$ with α.

Figure 29.- Effects of Reynolds number on the longitudinal aerodynamic characteristics of configuration BWVHN$_1$P$_1$ with $\delta_s = -0.23^0$, $i_n = 0.06^0$, $\Delta x/\bar{c} = 0$, and $\varepsilon = 0^0$. $M_\infty \approx 0.2$.

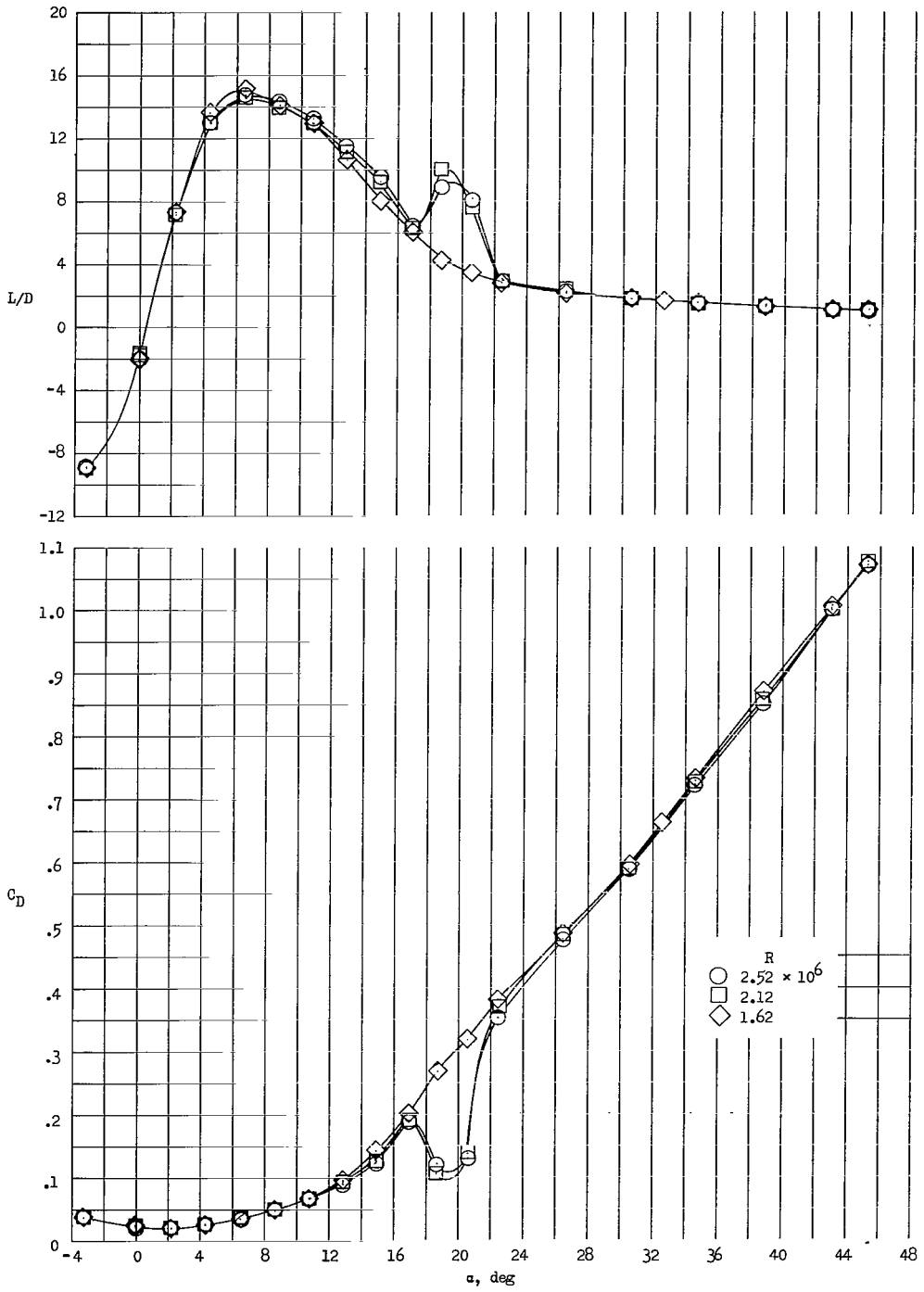

(b) Variation of C_D and L/D with α.

Figure 29.- Concluded.

"The aeronautical and space activities of the United States shall be conducted so as to contribute . . . to the expansion of human knowledge of phenomena in the atmosphere and space. The Administration shall provide for the widest practicable and appropriate dissemination of information concerning its activities and the results thereof."

—NATIONAL AERONAUTICS AND SPACE ACT OF 1958

NASA SCIENTIFIC AND TECHNICAL PUBLICATIONS

TECHNICAL REPORTS: Scientific and technical information considered important, complete, and a lasting contribution to existing knowledge.

TECHNICAL NOTES: Information less broad in scope but nevertheless of importance as a contribution to existing knowledge.

TECHNICAL MEMORANDUMS: Information receiving limited distribution because of preliminary data, security classification, or other reasons.

CONTRACTOR REPORTS: Technical information generated in connection with a NASA contract or grant and released under NASA auspices.

TECHNICAL TRANSLATIONS: Information published in a foreign language considered to merit NASA distribution in English.

TECHNICAL REPRINTS: Information derived from NASA activities and initially published in the form of journal articles.

SPECIAL PUBLICATIONS: Information derived from or of value to NASA activities but not necessarily reporting the results of individual NASA-programmed scientific efforts. Publications include conference proceedings, monographs, data compilations, handbooks, sourcebooks, and special bibliographies.

Details on the availability of these publications may be obtained from:

SCIENTIFIC AND TECHNICAL INFORMATION DIVISION

NATIONAL AERONAUTICS AND SPACE ADMINISTRATION

Washington, D.C. 20546